

WFA 86/05/28
MWC 86/06/27

Bohle

SANDIA REPORT SAND85-0854 • Unlimited Release • UC-70
Printed February 1986

Nevada Nuclear Waste Storage Investigations Project

The Effect of Percolation Rate On Water-Travel Time In Deep, Partially Saturated Zones

R. R. Peters, J. H. Gauthier, A. L. Dudley

Prepared by
Sandia National Laboratories
Albuquerque, New Mexico 87185 and Livermore, California 94550
for the United States Department of Energy
under Contract DE-AC04-76DP00789



HYDROLOGY DOCUMENT NUMBER 130

"Prepared by Nevada Nuclear Waste Storage Investigations (NNWSI) Project participants as part of the Civilian Radioactive Waste Management Program (CRWM). The NNWSI Project is managed by the Waste Management Project Office (WMPO) of the U. S. Department of Energy, Nevada Operations Office (DOE/NV). NNWSI Project work is sponsored by the Office of Geologic Repositories (OGR) of the DOE Office of Civilian Radioactive Waste Management (OCRWM)."

Issued by Sandia National Laboratories, operated for the United States Department of Energy by Sandia Corporation.

NOTICE: This report was prepared as an account of work sponsored by an agency of the United States Government. Neither the United States Government nor any agency thereof, nor any of their employees, nor any of their contractors, subcontractors, or their employees, makes any warranty, express or implied, or assumes any legal liability or responsibility for the accuracy, completeness, or usefulness of any information, apparatus, product, or process disclosed, or represents that its use would not infringe privately owned rights. Reference herein to any specific commercial product, process, or service by trade name, trademark, manufacturer, or otherwise, does not necessarily constitute or imply its endorsement, recommendation, or favoring by the United States Government, any agency thereof or any of their contractors or subcontractors. The views and opinions expressed herein do not necessarily state or reflect those of the United States Government, any agency thereof or any of their contractors or subcontractors.

Printed in the United States of America
Available from
National Technical Information Service
U.S. Department of Commerce
5285 Port Royal Road
Springfield, VA 22161

NTIS price codes
Printed copy: A03
Microfiche copy: A01

SAND85-0854C

THE EFFECT OF PERCOLATION RATE ON WATER-TRAVEL
TIME IN DEEP, PARTIALLY SATURATED ZONES*

by

R. R. Peters, J. H. Gauthier, and A. L. Dudley
Nevada Nuclear Waste Storage Investigations Project Department
Sandia National Laboratories
Albuquerque, New Mexico 87185

ABSTRACT

The Nevada Nuclear Waste Storage Investigations (NNWSI) project is investigating Yucca Mountain, Nye County, Nevada, as a prospective site for a radioactive-waste repository. The Yucca Mountain site is unique among those currently being investigated by the U.S. Department of Energy (DOE) in that the prospective repository location is in the unsaturated zone, approximately 300 m above the water table. The rock units at Yucca Mountain can be grouped into three types: (1) vitric tuffs with high matrix conductivity and few fractures, (2) zeolitized tuffs with low matrix conductivity and few fractures, and (3) densely welded tuffs with low matrix conductivities and many fractures. The prospective repository zone is in densely welded tuff; the units between it and the water table are of types 1 and 2.

Current percolation rates through Yucca Mountain, and those that are currently postulated under future climatic conditions, are thought to be of the order of the saturated matrix conductivity of some of the units. Although it is probable that there is now little or no water movement in fractures, it is necessary to investigate the potential for fracture flow, especially that which could be initiated under future climatic conditions. Significant fracture flow, if present, could reduce the water travel time between the repository and the water table.

A composite-porosity, continuum model was developed to model flow in a fractured, porous medium. Simulations using data from the Yucca Mountain site and this model in the one-dimensional code TOSPAC indicate that current estimates of the percolation rate result in water movement confined to the matrix and that the water-travel time from the repository to the water table is on the order of hundreds of thousands of years. This result is sensitive to the percolation rate; an increase in percolation rate of a factor of 10 may initiate water movement in the fractures, reducing the travel time significantly.

* This work, performed at Sandia National Laboratories, was supported by the U.S. Department of Energy under contract number DE-AC04-76DP0789.

TABLE OF CONTENTS

	<u>Page</u>
ABSTRACT	i
LIST OF FIGURES	iii
LIST OF TABLES	v
NOTATION	vi
INTRODUCTION	1
HYDROLOGIC CONCEPTUAL MODEL	1
MATHEMATICAL MODEL	5
HYDROLOGIC PROPERTIES	10
CALCULATIONAL CASE	13
RESULTS OF CALCULATIONS	18
Pressure-Head Solutions	18
Matrix Saturation	22
Water Velocity	24
Water Travel Time Across the Units at Yucca Mountain . . .	27
SUMMARY	33
REFERENCES	34

LIST OF FIGURES

<u>NO.</u>	<u>TITLE</u>	<u>Page</u>
1	Location of Yucca Mountain, Nevada Outline indicates preliminary repository boundary. Cross section in Fig. 2 is along line L-L'.	2
2	Conceptual model of flow at Yucca Mountain Cross section is along line L-L' in Fig. 1	2
3	Capacitance coefficients for Unit TSw2	14
4	Capacitance coefficients for Unit CHnv	14
5	Conductivity curve for Unit TSw2	15
6	Conductivity curve for Unit CHnv	15
7	One-dimensional column used in calculations	17
8	Pressure head versus distance above the water table for vitric unit CHn cases	19
9	Pressure head versus distance above the water table for zeolitized unit CHn cases	19
10	Relative percolation rate versus distance above the water table for vitric unit CHn cases; results are shown for three different percolation rates	20
11	Relative percolation rate versus distance above the water table for zeolitized unit CHn cases; results are shown for three different percolation rates	20
12	Matrix saturation versus distance above the water table for vitric unit CHn cases	23
13	Matrix saturation versus distance above the water table for zeolitized unit CHn cases	23
14	Water velocity in the matrix versus distance above the water table for vitric unit CHn cases	25
15	Water velocity in the matrix versus distance above the water table for zeolitized unit CHn cases	25
16	Water velocity in the fractures versus distance above the water table for vitric unit CHn cases	26

LIST OF FIGURES CONT'D

<u>NO.</u>	<u>TITLE</u>	<u>Page</u>
17	Water velocity in the fractures versus distance above the water table for zeolitized unit CHn cases	26
18	Water travel time across the units at Yucca Mountain for a vitric unit CHn and a percolation rate of 0.1 mm/yr	28
19	Water travel time across the units at Yucca Mountain for a zeolitized unit CHn and a percolation rate of 0.1 mm/yr . .	28
20	Water travel time across the units at Yucca Mountain for a vitric unit CHn and a percolation rate of 0.5 mm/yr	29
21	Water travel time across the units at Yucca Mountain for a zeolitized unit CHn and a percolation rate of 0.5 mm/yr . .	29
22	Water travel time across the units at Yucca Mountain for a vitric unit CHn and a percolation rate of 4.0 mm/yr	30
23	Water travel time across the units at Yucca Mountain for a zeolitized unit CHn and a percolation rate of 4.0 mm/yr . .	30

LIST OF TABLES

<u>NO.</u>	<u>TITLE</u>	<u>Page</u>
1	Unsaturated zone, hydrologic unit properties	11
2	Calculation case definition	16
3	Water travel time from the prospective repository location to the water table	32

NOTATION

- $\frac{dn_f}{d\sigma'}$ - the compressibility of the fracture porosity (1/m)
- \bar{K} - the hydraulic conductivity (m/s)
- n - the porosity
- \bar{q} - specific discharge (m/s)
- S - the saturation as a function of pressure head
- t - time (s)
- T - time for water to travel some specified distance (s)
- \bar{V} - water velocity (m/s)
- z - elevation above arbitrary reference plane (m)

Greek Symbols

- α - a curve-fitting parameter in Eq. 4
- α'_{bulk} - the coefficient of consolidation of the medium (1/m)
- B - a curve-fitting parameter in Eq. 4
- B'_w - the water compressibility (1/m)
- ψ - the pressure head (m of water)
- ρ - the density of water (kg/m³)
- σ - rock stress (m)

Subscripts

- f - fractures
- f,b - bulk fracture
- f,r - value in fractures at residual saturation
- m - matrix
- m,b - bulk matrix
- m,r - value in matrix at residual saturation
- r - value at residual saturation
- s - value at full saturation

INTRODUCTION

The emplacement of radioactive waste in the partially saturated zone above the water table is being investigated as a possible solution to the problem of isolating the waste from the biosphere for a very long time. Several authors have discussed the relative merits of emplacing nuclear waste in the unsaturated zone rather than in the saturated zone below the water table (e.g., Mercer, 1983; Roseboom, 1983; and Winograd, 1981). Currently, the U.S. Department of Energy (DOE) is studying the geological formations in the unsaturated zone in Yucca Mountain, on and adjacent to the Nevada Test Site (NTS); these studies are being performed by the Nevada Nuclear Waste Storage Investigations (NNWSI) project. The purpose of this paper is to discuss, in general, the hydrologic system of the Yucca Mountain site and to discuss in some detail the percolation rate and its significant influence on the mechanism and rate of water movement in Yucca Mountain. The paper discusses in order (1) the hydrologic conceptual model, (2) the mathematical model consistent with the mechanisms discussed in the hydrologic conceptual model, (3) the hydrologic data available for Yucca Mountain, (4) the definition of the calculational cases, and (5) the results of these calculations.

HYDROLOGIC CONCEPTUAL MODEL

The geology and climate of Yucca Mountain have a significant influence on the hydrologic system of Yucca Mountain. Yucca Mountain (Figure 1) lies within the Basin and Range physiographic province characterized by generally linear mountain ranges and intervening valleys. Yucca Mountain is a prominent group of north-trending, fault-block ridges. The elevation of northern Yucca Mountain is approximately 1500 m. The ridge of Yucca Mountain is about 300 m above the surrounding valley floors.

Yucca Mountain is made up predominantly of ashflow and ashfall tuffs. These may be organized into hydrologic units which have property variations which are small compared to the differences in properties between units. Figure 2 shows an east-west cross section through

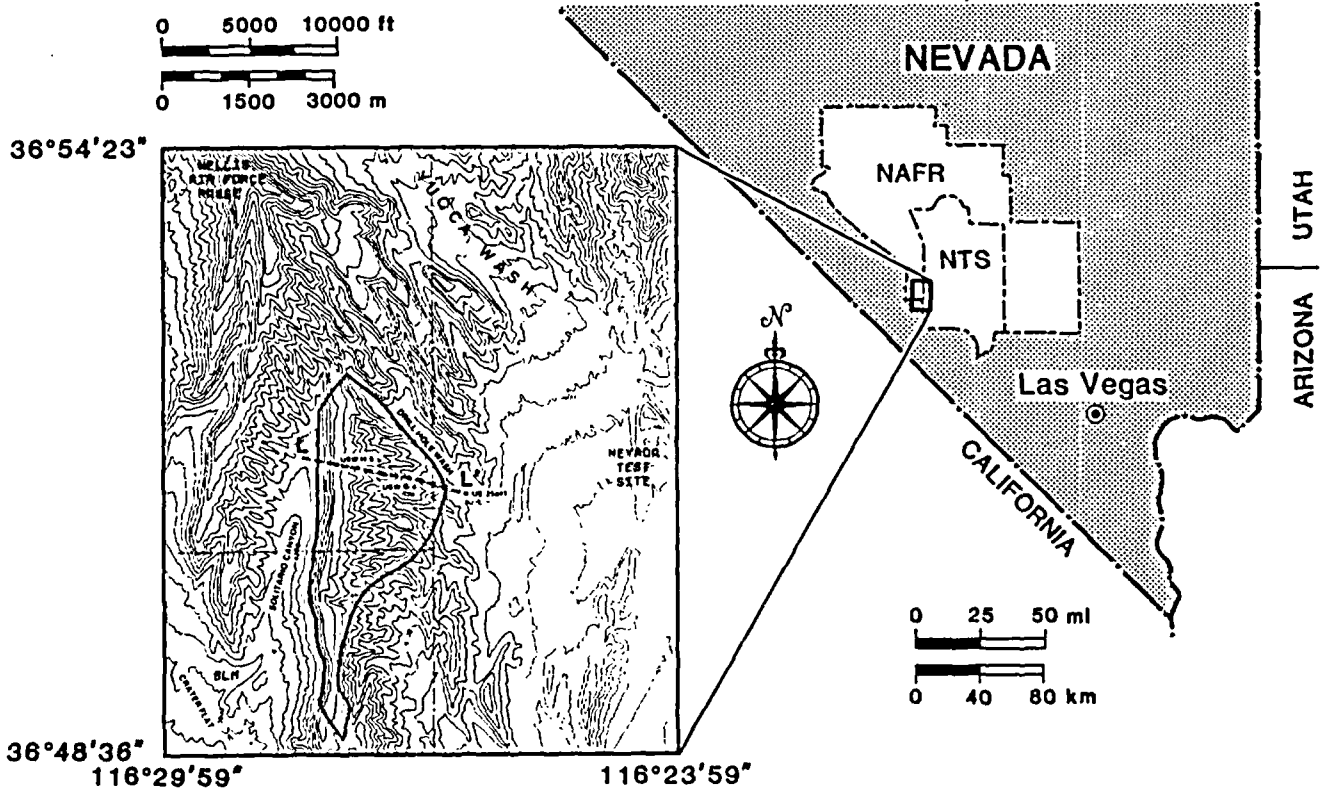


Figure 1. Location of Yucca Mountain, Nevada
 Outline indicates preliminary repository boundary
 Cross section in Fig. 2 is along line L-L'

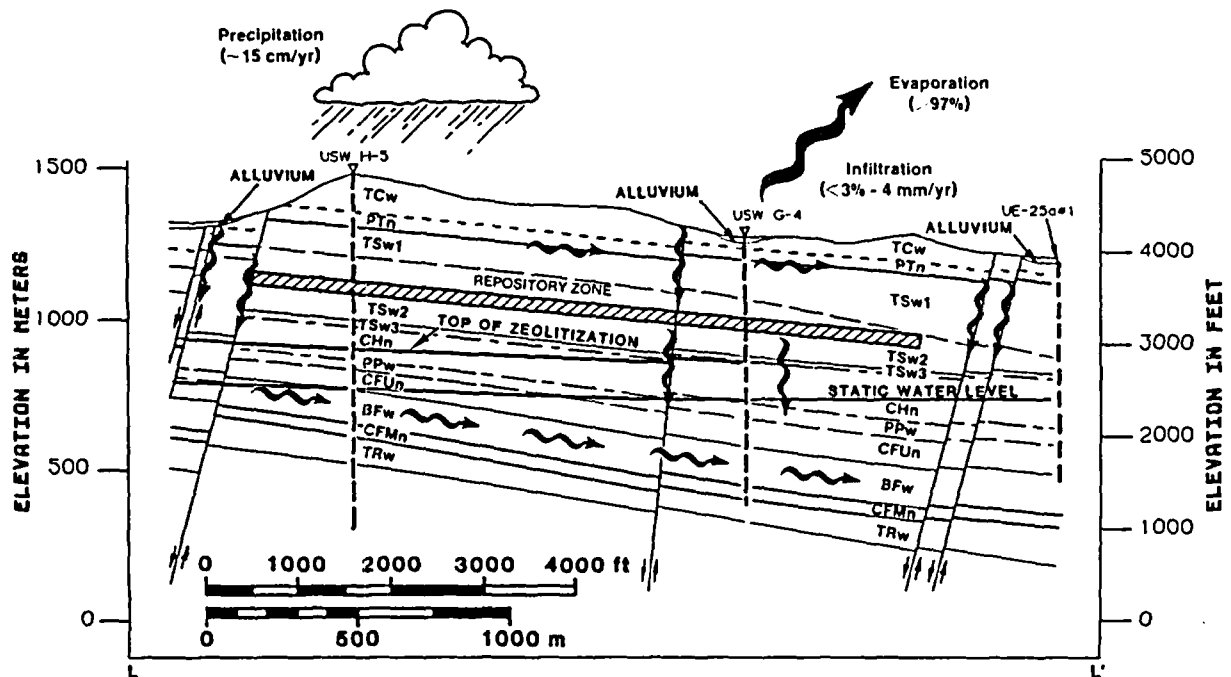


Figure 2. Conceptual model of flow at Yucca Mountain
 Cross section is along line L-L' in Fig. 1

Yucca Mountain with the location of the hydrologic units and the water table indicated (Ortiz et al., 1985). All but two of the units have fairly constant thicknesses in this cross section. Unit TCw has variable thickness as a result of surface erosion. At most locations at Yucca Mountain, unit CHn consists of a layer of vitric material (denoted as unit CHnv) on top of a layer of zeolitized material (denoted as unit CHnz) with the thickness of each ranging from near zero to approximately 100% of the total thickness of unit CHn. The hydrologic units may be organized into three basic groups:

1) Densely welded tuffs that are highly fractured.

These units have low saturated matrix conductivities (10^{-11} m/s or less) and high saturated fracture conductivities (for a unit volume of rock, the total saturated conductivity of the fracture system is probably several orders of magnitude higher than the total saturated conductivity of the matrix). The units included in this group are TCw, TSw1, TSw2 and TSw3.

2) Nonwelded, vitric tuffs that have few fractures.

These units have high saturated matrix conductivities (in the range of about 10^{-6} to 10^{-8} m/s) and saturated fracture conductivities that are less than the saturated matrix conductivity. The units included in this group are PTn and CHnv (the vitric portion of unit CHn).

3) Nonwelded, zeolitized tuffs that have few fractures.

These units have low saturated matrix conductivities (10^{-11} m/s or less) and saturated fracture conductivities that are somewhat larger than the saturated matrix conductivity but less than the saturated conductivity of fractures found in densely welded tuffs. The unit above the water table included in this group is CHnz (the zeolitized portion of unit CHn).

Yucca Mountain is located in an arid region with a very deep water table. The annual precipitation on Yucca Mountain is approximately 150 mm. The infiltration (the flux of downward-moving water at a depth of

several meters) into Yucca Mountain is thought to be small [less than 4.5 mm/yr (1.3×10^{-10} m/s) according to the Draft Environmental Assessment (DOE, 1984, pp. 6-136)] which bases its conclusion on work by Rush (1970) and others. The possible flow paths for this water (Figure 2) are highly dependent upon the percolation rate (i.e., the water flux at depth) in each unit. The percolation rate in the lower units may be lower than the infiltration rate primarily because of lateral diversion of the water at interfaces between units (indicated schematically in the figure). The currently postulated percolation rate in the prospective repository unit and in those between it and the water table is less than 1.0 mm/yr and is likely to be less than 0.2 mm/yr (DOE, 1984, pp. 6-136). The higher percolation rate (1.0 mm/yr) is approximately the same as the matrix rock conductivity of the least-conductive units. The lower value is less than the matrix conductivity of the least conductive units. Thus, it is thought that essentially no water movement in fractures should occur because capillary forces will cause the water to remain within the small pores of the matrix as long as matrix conductivity is not excluded, i.e., as long as the matrix does not become saturated. However, one currently suggested upper bound of the steady-state percolation rate (<4.5 mm/yr in DOE (1984), pp. 6-136 based on Rush (1970)) is greater than the matrix conductivity of some units. Therefore, in the steady state with the upper-bound value of percolation rate, water may move in both the fractures and the matrix in some units (e.g., unit TSw2, the unit proposed as the host for repository). The calculations discussed in this paper assume that the percolation rate is the same in each unit and no lateral water diversion occurs at unit interfaces.

The movement of water vapor upward through the mountain may be a significant mechanism for the movement of water at Yucca Mountain (Montazer and Wilson, 1984) because the percolation rate is thought to be small. Calculations by Ross (1984) indicate an upper bound on the upward movement of vapor flux (driven by the geothermal gradient) is about 0.03 mm/yr. This value is less than the lowest value of percolation rate considered in this paper. Upward movement of water vapor has not yet been included in the mathematical model and the computer code used in these calculations (TOSPAC, Dudley et al., in preparation). Therefore, vapor transport is not considered in this paper.

MATHEMATICAL MODEL

The use of porous-media models is not appropriate for water flow calculations in some units because, under some sets of conditions that are thought to exist now, it is possible that the fractures and the matrix material carry comparable quantities of water. However, the use of codes that explicitly take into account the fractures is not practical because there may be of the order of 10^{10} fractures in a site-scale problem. The results of hydrologic calculations by two investigators (Travis et al., 1984; Martinez, in preparation) suggest that episodic pulses of water probably will not penetrate to great depths except near large structural features like faults or in regions where the fractures have very large apertures (of the order of several millimeters). The water in the fractures, due to episodic pulses, quickly moves into the matrix for conditions thought to be representative of Yucca Mountain.

Wang and Narasimhan (1985) used the TRUST computer code to investigate the movement of water in a rock mass where the fractures were explicitly zoned into the rock mass. The results of their calculations indicate that the pressure heads in the fractures and in the matrix are nearly identical under drainage conditions, a condition where the flux is changing fairly slowly in time. Thus, at depth, where the results of both Travis and Martinez indicate that the water flux is a slowly varying function of time, it is likely (according to the work of Wang and Narasimhan) that the matrix and fracture pressure heads are identical. The matrix and fracture pressure heads are likely to be nearly identical at many other locations, besides Yucca Mountain, where the water flux is a slowly varying function of time.

The following information and assumptions were used to derive the flow equation that describes the movement of water in a fractured, rock mass:

- 1) The continuity equation for the material making up the matrix (the rock grains).
- 2) The three-dimensional bulk rock consolidation equation with the assumption that the displacement is vertical [see Reeves and Duguid (1975) for further discussion].

- 3) The assumption that a unit change in the quantity "total saturation times pressure head" at a point causes a unit change in the local stress field [see McTigue, Wilson, and Nunziato (1984)].
- 4) The assumption that the fluid flow may be calculated using Darcy's equation.
- 5) The assumption that the pressure heads in the fractures and the matrix are identical in a direction perpendicular to the flow lines.
- 6) The conventional definition of the total head as the sum of the pressure head and the elevation above some reference surface.

This flow equation may be used to calculate the pressure-head field in a fractured, porous medium. The pressure-head field may then be used to calculate the flow field, saturation distribution in the rock matrix and the fractures, etc. using the equations which follow. The derivation of Eq. 1 is presented by Klavetter and Peters (1985b) and only the final result is presented here.

$$\begin{aligned}
 & \rho \frac{\partial \psi}{\partial t} \left[n_m \frac{\partial S_m}{\partial \psi} + n_f \frac{\partial S_f}{\partial \psi} \beta_w' (S_m n_m + S_f n_f) + \right. \\
 & \left. - \alpha_{\text{bulk}}' \left(\frac{(S_m n_m + S_f n_f)}{n_m + n_f} \right) \left[(S_m - n_f (S_m - S_f)) \right] \right] - \quad (1) \\
 & - \frac{\partial n_f}{\partial \sigma'} \left(\frac{(S_m n_m + S_f n_f)}{n_m + n_f} \right) (S_m - S_f) \Big] = \nabla \cdot \left(\rho (\bar{K}_{m,b} + \bar{K}_{f,b}) \cdot \nabla (\psi + z) \right)
 \end{aligned}$$

where:

α_{bulk}' - the coefficient of consolidation of the medium (1/m)

β_w' - the water compressibility (1/m)

ρ - the density of water (kg/m^3)

ψ - the pressure head (m)

n - the porosity

$\frac{dn_f}{d\sigma'}$ - the compressibility of the fracture porosity with " σ " being defined as the rock stress (1/m)

t - time (s)

z - elevation above an arbitrary reference plane (m)

The subscripts "m" and "f" refer to matrix and fracture respectively. The subscripts "m,b" and "f,b" refer to bulk matrix and bulk fractures. The bulk conductivity of a particular material is the material conductivity times its relative volume. The bulk fracture conductivity and bulk matrix conductivity in a vertical direction are defined below.

$$K_{f,b} = n_f K_f \quad (2)$$

$$K_{m,b} = (1 - n_f) K_m \approx K_m \quad (3)$$

n_f is of the order of 10^{-5} . Therefore, " $1 - n_f$ " is approximately equal to 1.

The saturation function "S" and the scalar hydraulic conductivity function "K" in Eq. 1 are complicated functions of " ψ " that are defined below.

S - the saturation as a function of pressure head. The functional form used for these calculations was developed by van Genuchten (1978).

$$S(\psi) = (S_s - S_r) \left(\frac{1}{1 + |\alpha\psi|^\beta} \right)^\lambda + S_r \quad (4)$$

The variables in Eq. 4 are defined as follows.

S_s - the saturation at the fully saturated state (~1)

S_r - the residual saturation

α - a curve-fitting parameter that primarily affects the pressure head at which desaturation begins.

β - a curve-fitting parameter that primarily affects the slope of the desaturation portion of the curve.

$$\lambda = 1 - 1/\beta \quad (5)$$

K - the hydraulic conductivity. The hydraulic conductivity is a function of pressure head. The functional form used in these calculations was developed by Mualem (1976).

$$K(\psi) = K_s \left(1 + |\alpha\psi|^\beta \right)^{-\lambda/2} \left(1 - \frac{|\alpha\psi|^\beta}{1 + |\alpha\psi|^\beta} \right)^{\lambda/2} \quad (6)$$

K_s - the saturated conductivity.

The steady-state pressure-head field is calculated by a Darcy's law equation where \bar{q} is the flux.

$$- [\bar{K}_{m,b} + \bar{K}_{f,b}] \cdot \nabla(\psi + z) = \bar{q}_m + \bar{q}_f = \bar{q}_{total} \quad (7)$$

The pressure-head field may then be used to calculate the flow field, etc. The steady-state module of the TOSPAC code solved Eq. 7 for the one-dimensional movement of water. Most other codes (e.g., TRUST (Reisenauer et al., 1982)) are designed to solve an equation associated with unsteady flow of water (some form of Richards' equation (Richards, 1931)) and thus, would use Eq. 1. The unsteady-flow module of TOSPAC solves Eq. 1.

The average linear velocity of the water movement in the matrix and in the fractures is necessary for determining quantities for which Environmental Protection Agency (EPA) and Nuclear Regulatory Commission (NRC) guidelines exist: (1) the travel time of water from the repository to the accessible environment and (2) the rates at which radionuclides move into the accessible environment. The water velocities in matrix and fractures were calculated in the manner shown below. The water velocity is the Darcy flux divided by the area through which the water moves. The saturations and fluxes are functions of the pressure head which is determined by the solution of either Eq. 1 or 7.

$$\bar{V}_m = \bar{q}_m / [n_m (S_m - S_{m,r})] = - \bar{K}_{m,b} \cdot \nabla (\psi + z) / [n_m (S_m - S_{m,r})] \quad (8)$$

$$\bar{V}_f = \bar{q}_f / [n_f (S_f - S_{f,r})] = - \bar{K}_{f,b} \cdot \nabla (\psi + z) / [n_f (S_f - S_{f,r})] \quad (9)$$

$S_{m,r}$ and $S_{f,r}$ are the residual saturations of the matrix and fractures, respectively.

The equation used to calculate the time (T) required for water to travel across one of the hydrologic units (or some other distance) is listed below.

$$T = \int_{z_L}^{z_U} dz/V \quad (10)$$

z_u and z_L are, respectively, the elevations of the upper and lower boundaries. The water velocity in Eq. 10 may be the matrix water velocity, the fracture water velocity, or some combination of the two and may be highly variable both within a unit and as a unit boundary is crossed. Three different kinds of travel times result from the use of (1) only the matrix water velocity [matrix water travel time], (2) only the fracture water velocity [fracture water travel time], and (3) the maximum water velocity (the velocity used in this calculation would be the fracture velocity where there is significant water movement in the fractures and the matrix water velocity in the remainder) [minimum travel time]. Because the fracture water velocity may be zero in part or all of a particular unit, in some calculations it may be impossible to define the fracture water travel time across the entire unit. When such results are reported below, a notation will be made that either the value is undefined (and labeled "N/A" (not applicable)) or, if flow occurs across a portion of the unit, a notation will be made telling the fraction of the unit water can cross in the fractures and the time required to cross that portion of the unit.

HYDROLOGIC PROPERTIES

The values of the physical parameters used in these calculations are based on a variety of sources including reports by Peters et al.(1984), Scott et al.(1983), and Sinnock et al.(1984). The values used in the calculations are listed in Table 1; footnotes give the sources of the data.

Table 1. Unsaturated Zone, Hydrologic Unit Properties

Unit	Sample Code	Matrix Properties ^a					
		Grain Density	Porosity	Hydraulic Conductivity	S_r	α	β
		(g/cm ³)	{n _m }	{K _{m,b} } (m/s)		(10 ⁻² /m)	
TCw	G4-1	2.49	0.08	9.7 x 10 ⁻¹²	0.002	0.821	1.558
FTn	GU3-7	2.35	0.40	3.9 x 10 ⁻⁰⁷	0.100	1.50	6.872
TSw1	G4-6	2.58	0.11	1.8 x 10 ⁻¹¹	0.080	0.567	1.798
TSw2-3	G4-6	2.58	0.11	1.8 x 10 ⁻¹¹	0.080	0.567	1.798
CHnv	GU3-14	2.37	0.46	2.7 x 10 ⁻⁰⁷	0.041	1.60	3.872
CHnz	G4-11	2.23	0.28	2.0 x 10 ⁻¹¹	0.110	0.308	1.602

Unit	Sample Code	Fracture Properties ^c						
		Horizontal Stress ^d	Fracture Aperture	Fracture Conductivity	Fracture Density ^e	Fracture Porosity ^f	Fracture Compressibility	Bulk Frac. Conductivity ^g
		(bars)	(microns)	(10 ⁻⁵ m/s)	(No./m ³)	{n _f } (10 ⁻⁵)	{ $\partial n_f / \partial \sigma'$ } (10 ⁻⁸ /m)	{K _{f,b} } (10 ⁻⁹ m/s)
TCw	G4-2F	1.1	6.74	3.8	20	14.	132.	5.3
FTn	G4-3F	3.3	27.0	61.	1	2.7	19.	16.
TSw1	G4-2F	9.5	5.13	2.2	8	4.1	5.6	0.90
TSw2-3	G4-2F	21.9	4.55	1.7	40	18.	12.	3.1
CHnv	G4-4F	34.3	15.5	20.	3	4.6	2.8	9.2
CHnz	G4-4F	34.3	15.5	20.	3	4.6	2.8	9.2

Fracture saturation coefficients are $S_r = 0.0395$, $\alpha = 1.2851/m$, and $\beta = 4.23$

Unit	TCw	FTn	TSw1	TSw2-3	CHnv	CHnz
Coefficient of consolidation ^h { α'_{bulk} } (10 ⁻⁷ /m)	6.2	82.	12.	5.8	39.	26.

The compressibility of water { β'_w } is $9.8 \times 10^{-7}/m$

- Notes: a) All matrix data in this section are from Peters et al. (1984).
 b) The matrix saturated conductivity and the bulk matrix saturated conductivity (K_{m,b}) are essentially the same because the factor that converts the matrix value to the bulk matrix value (1-n_f) is nearly equal to 1.0
 c) Unless noted otherwise, this fracture information is from Peters et al. (1984).
 d) Horizontal stress assumed to be one-third the overburden weight, evaluated at average unit depth in USW G-4.
 e) Based on the report by Scott et al. (1983).
 f) Calculated as fracture volume (aperture times 1 square meter) times number of fractures per cubic meter.
 g) This value of "K_{f,b}" was obtained by multiplying the fracture conductivity by the fracture porosity.
 h) Based on the report by Nimick et al. (1984).

The values listed in Table 1 are, with one exception, based on physical measurements. The exception is the fracture saturation curve; information regarding fracture saturation characteristics is scarce. Wang and Narasimhan (1985) have used statistical concepts to develop equations describing the saturation curve for fractures in a densely welded tuff. Their fracture saturation curve is similar to that of a coarse sand such as that shown in Freeze and Cherry's text (1979, p. 42). Plans are being made to measure the saturation curves of fractured core experimentally (Klavetter, Peters, and Schwartz, 1985). The coefficients of the assumed fracture saturation curve (based on the Freeze and Cherry sand curve), the saturated fracture conductivity, and Eq. 6 were used to calculate the fracture conductivity curve used in these calculations.

Most codes would solve Eq. 1 to obtain the steady-state movement of water for these problems. Therefore, a discussion of the physical meaning of the coefficients in Eq. 1 and their curve shape and value is relevant to those who may wish to reproduce these results. For convenience in discussion and labeling of the plots, the mathematical terms in the left side of Eq. 1 are named as follows.

$$\text{Matrix Sat.:} \quad n_m \frac{\partial S_m}{\partial \psi}$$

$$\text{Fracture Sat.:} \quad n_f \frac{\partial S_f}{\partial \psi}$$

$$\text{Water Comp.:} \quad \beta_w (S_m n_m + S_f n_f)$$

$$\text{Bulk Rock Comp.:} \quad \alpha_{\text{bulk}} \left(\frac{[S_m n_m + S_f n_f]}{n_m + n_f} \right) [S_m - n_f (S_m - S_f)] \approx \alpha_{\text{bulk}} S_m^2$$

$$\text{Fracture Comp.:} \quad \frac{\partial n_f}{\partial \sigma'} \left(\frac{(S_m n_m + S_f n_f)}{n_m + n_f} \right) (S_m - S_f) \approx \frac{\partial n_f}{\partial \sigma'} S_m (S_m - S_f)$$

The coefficients on the left side of Eq. 1 (referred to as "capacitance coefficients") relate to the storage of water as " ψ " is varied. The first two terms on the left side (named above as Matrix Sat. and Fracture Sat.) correspond to the storage of water in the unit volume due to saturation of the matrix and the fracture system. The second group (named above as Water Comp.) corresponds to the storage of water due to the compressibility of water contained in the fractured, porous medium. The final group on the left side (Bulk Rock Comp. and Fracture Comp.) represents the storage of water due to dilation of the bulk rock. The term on the right side is proportional to the divergence of the total water flux moving through the unit volume.

The capacitance coefficients found in Eq. 1 have a strong functional dependence on the pressure head. Plots of the functional dependence of the capacitance coefficients on pressure head are shown in Figures 3 and 4 for the unit that is the prospective location for the repository and for a unit below it.

Fracture conductivity and matrix conductivity are also highly variable with pressure head because of changes in the saturation of the matrix and the fractures. The conductivity curves for the fractures, the matrix material, and a unit volume containing both fractures and matrix ($K_{fb} + K_{mb}$) are shown in Figures 5 and 6 for the same two units as shown in the figures for the capacitance coefficients. A detailed discussion of the functional dependence of the capacitance coefficients and the conductivity on the pressure head will be given by Klavetter and Peters (1985b) and is given in another paper being presented at this conference (Klavetter and Peters, 1985a).

CALCULATIONAL CASES

The groundwater velocity, water flow time across the units which make up Yucca Mountain, and other pertinent parameters were determined as a function of the percolation rate and composition of unit CHn; Table 2 lists the specific calculational cases investigated. The calculational

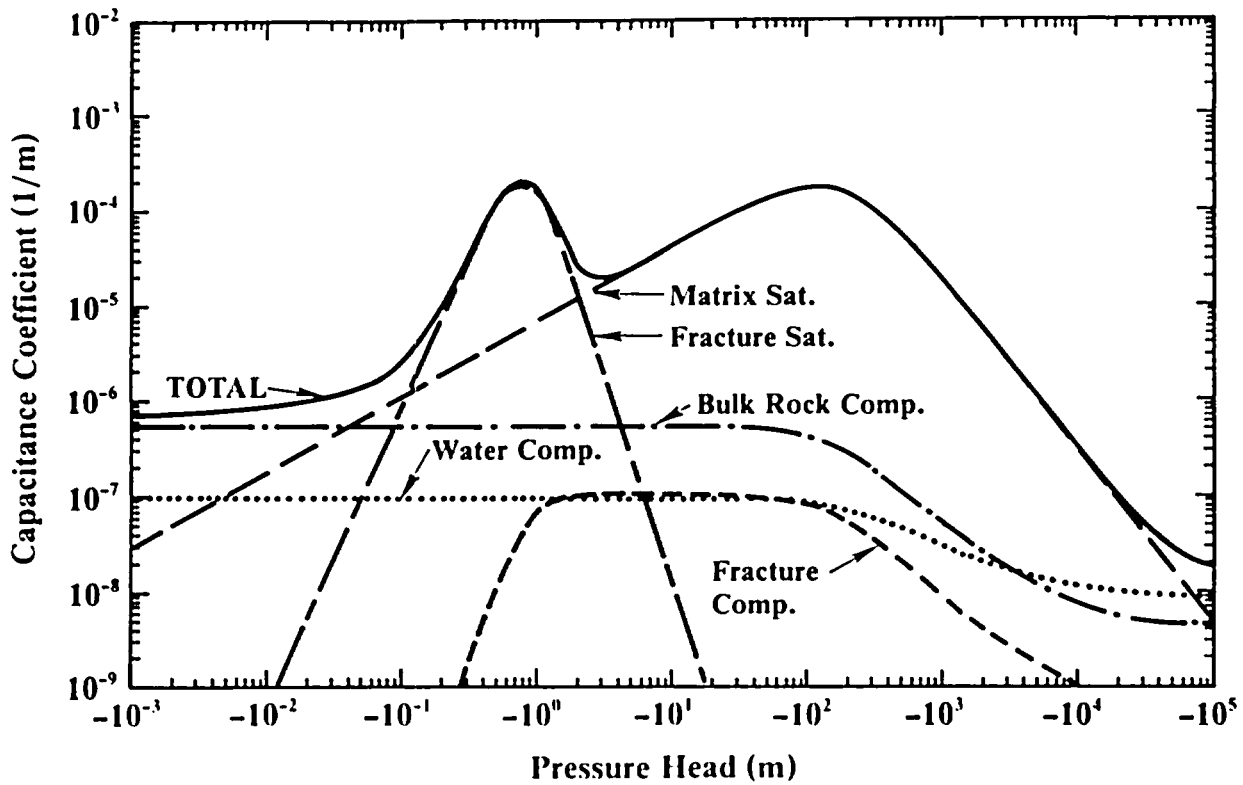


Figure 3. Capacitance coefficients for Unit TSw2

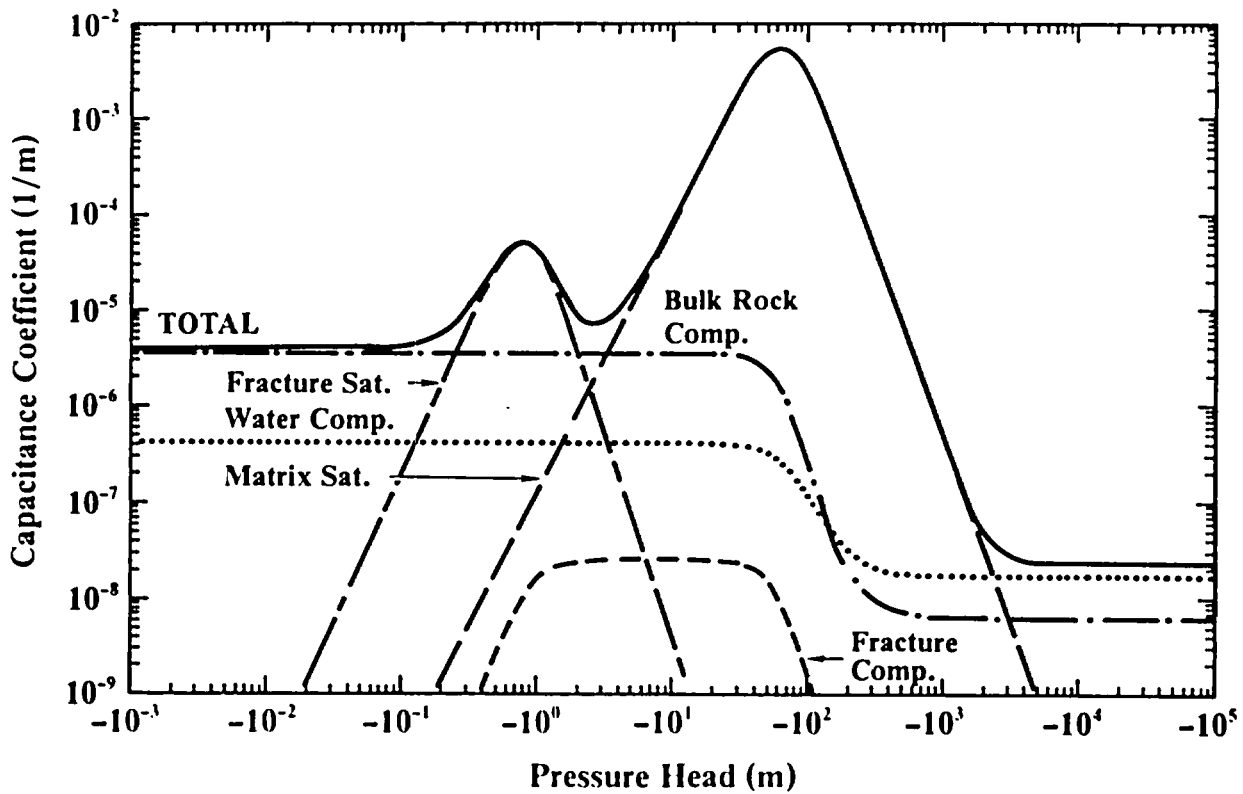


Figure 4. Capacitance coefficients for Unit CHnv

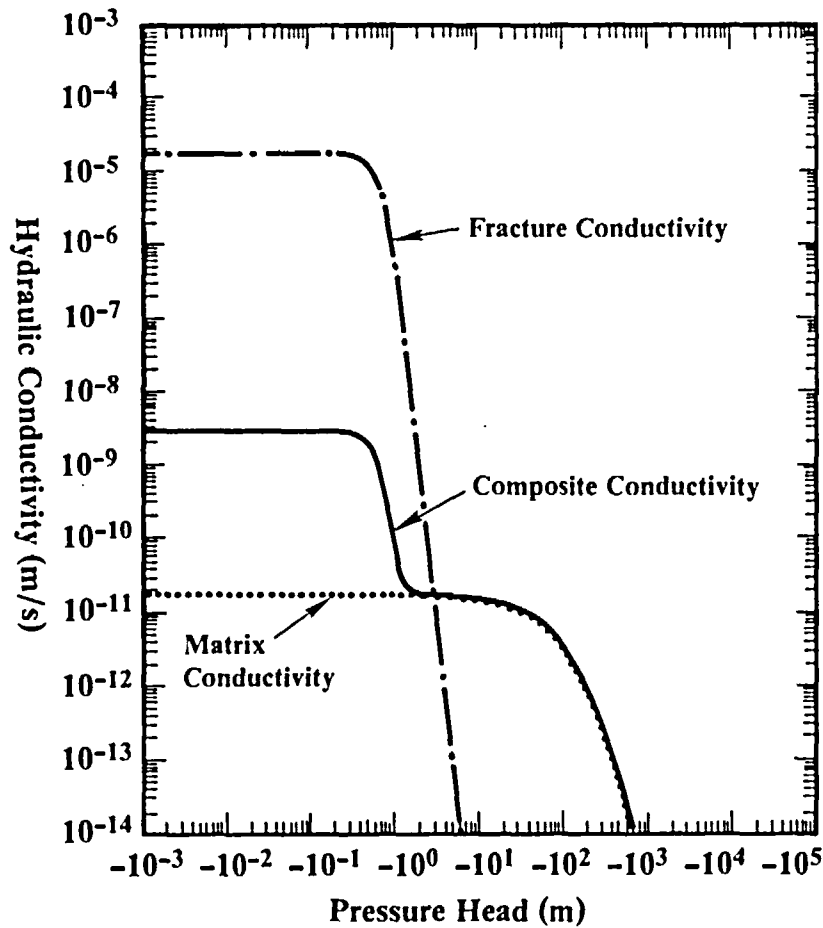


Figure 5. Conductivity curve for Unit TSw2

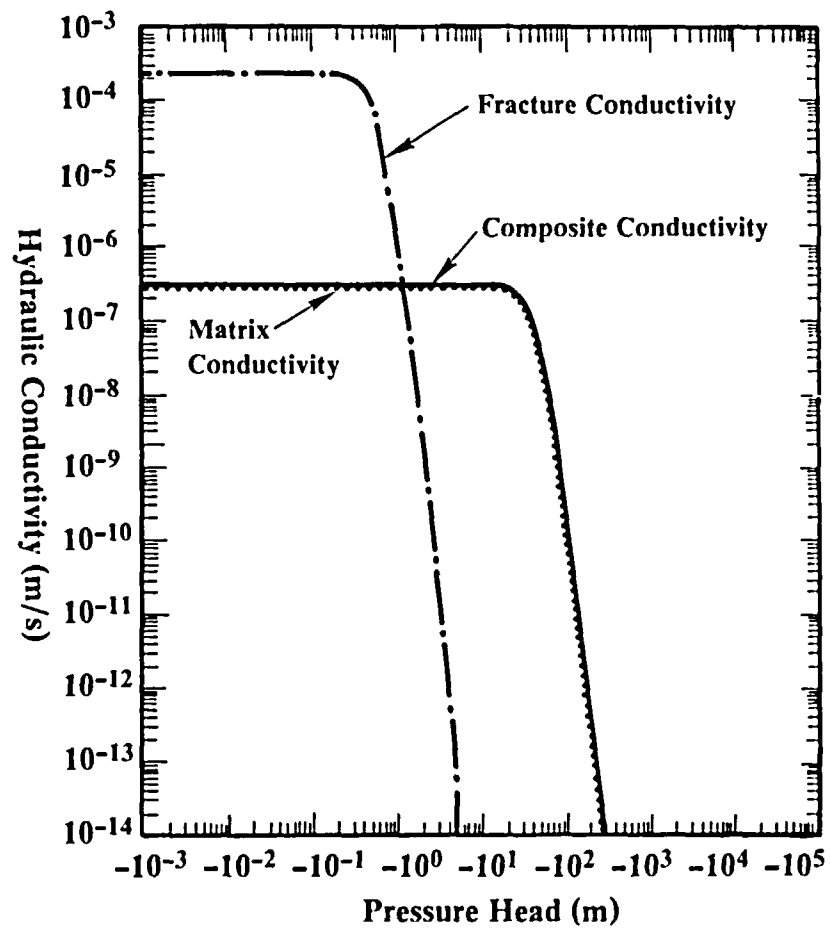


Figure 6. Conductivity curve for Unit CHnv

Table 2 Calculation case definition

<u>CASE</u>	<u>PERCOLATION RATE</u> <u>(mm/yr)</u>	<u>CHn MATERIAL</u>
1	0.1	Vitric, CHnv properties
2	0.1	Zeolitic, CHnz properties
3	0.5	Vitric, CHnv properties
4	0.5	Zeolitic, CHnz properties
5	4.0	Vitric, CHnv properties
6	4.0	Zeolitic, CHnz properties

set has two cases for the composition of unit CHn that correspond to the extremes that may be found at Yucca Mountain; either it is vitric with a relatively high conductivity (the unit is then referred to as CHnv), or it is zeolitized with a relatively low conductivity (the unit is then referred to as CHnz). The relative elevations of each of the units used in the one-dimensional calculations (Figure 7) are based on the stratigraphy of drill hole USW G-4, which is located on the eastern boundary of the prospective repository location (Figures 1 and 2). Unit TSw3 is combined with TSw2 in this column because it is relatively thin (~15 m) and has rock mass hydrologic properties similar to those of TSw2. The combined unit is referred to as "TSw2-3". These calculations assume that the unit properties are constant throughout each unit.

The percolation rate values listed in Table 2 span the range suggested for the Yucca Mountain site under current conditions and under currently postulated future scenarios (DOE, 1984). As shown below, these values also span the range over which water movement occurs only in the matrix and in both the matrix and the fractures. The cases having a percolation rate of 0.1 mm/yr have water movement only in the matrix nearly everywhere in the column. The 0.5-mm/yr problems have a relatively small amount of water movement in the fractures in some units. The 4.0-mm/yr problems have considerable water movement in fractures in some units (e.g., units TCw and TSw2-3).

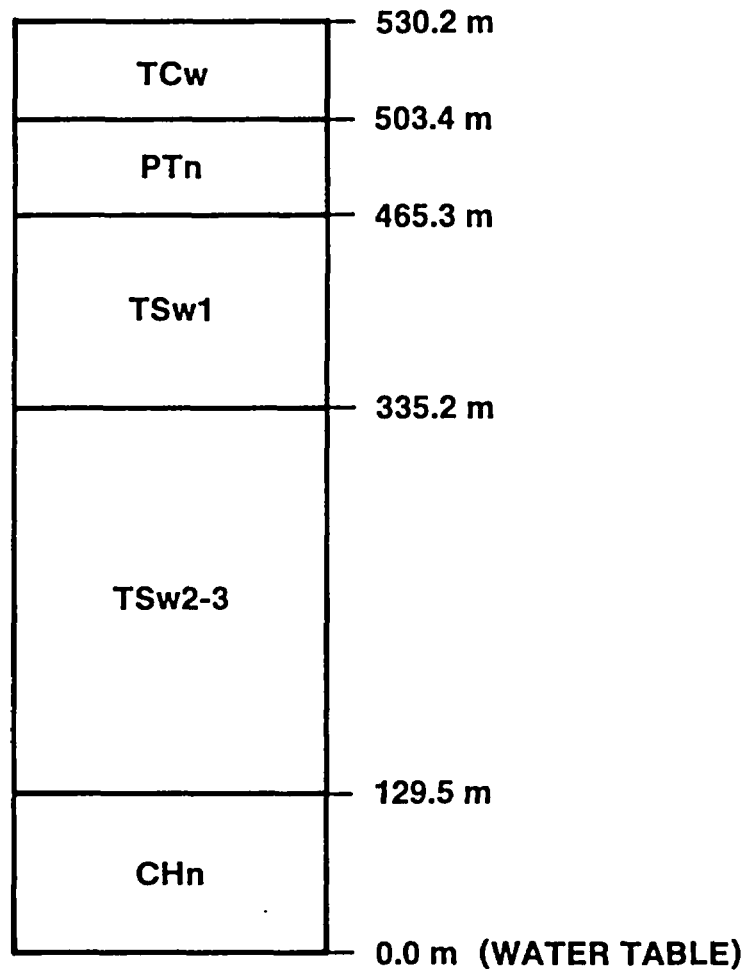


Figure 7. One-dimensional column used in calculations

RESULTS OF CALCULATIONS

The six steady-state problems listed in Table 2 have been solved using TOSPAC. The results concerning a particular variable (e.g., the pressure-head profile) will be discussed for cases where unit CHn is vitric and the percolation rate is varied. These results will then be compared to those where unit CHn is zeolitized to illustrate the effect of changing the composition of one unit.

Pressure-Head Solutions

The solutions to Eq. 7 for the six different cases are shown in Figures 8 and 9. Figure 8 shows the unit CHnv pressure-head profiles for three different percolation rates and Figure 9 shows the CHnz pressure-head profiles. The first matter to be considered is the accuracy of these solutions. This was checked by calculating the percolation rate at each node point using the pressure-head solution, the physical properties, and Eq. 7. Very slight errors in the pressure-head solution can cause major errors in the calculated percolation rate, especially if the water movement is primarily in the fractures. Thus, the calculated percolation rate is a very sensitive measure of the accuracy of the pressure-head solution. The calculated percolation rate (Figures 10 and 11) is plotted as relative percolation rate, which is the percolation rate at a point divided by the imposed percolation rate. Figure 10 indicates that the solutions are accurate in terms of this sensitive measure. The relative percolation rates for the cases where unit CHn is zeolitized (Figure 11) also show that good solutions were obtained.

The steady-state pressure-head solution is a function of the percolation rate, the conductivity and the pressure head boundary conditions. In general, the pressure head decreases to large negative values as the percolation rate is decreased. If the matrix conductivity of a unit is small when compared to the percolation rate (e.g., the case where a percolation rate of 4.0 mm/yr passes through unit TSw2-3, which has a saturated matrix conductivity of about 0.6 mm/yr), then the

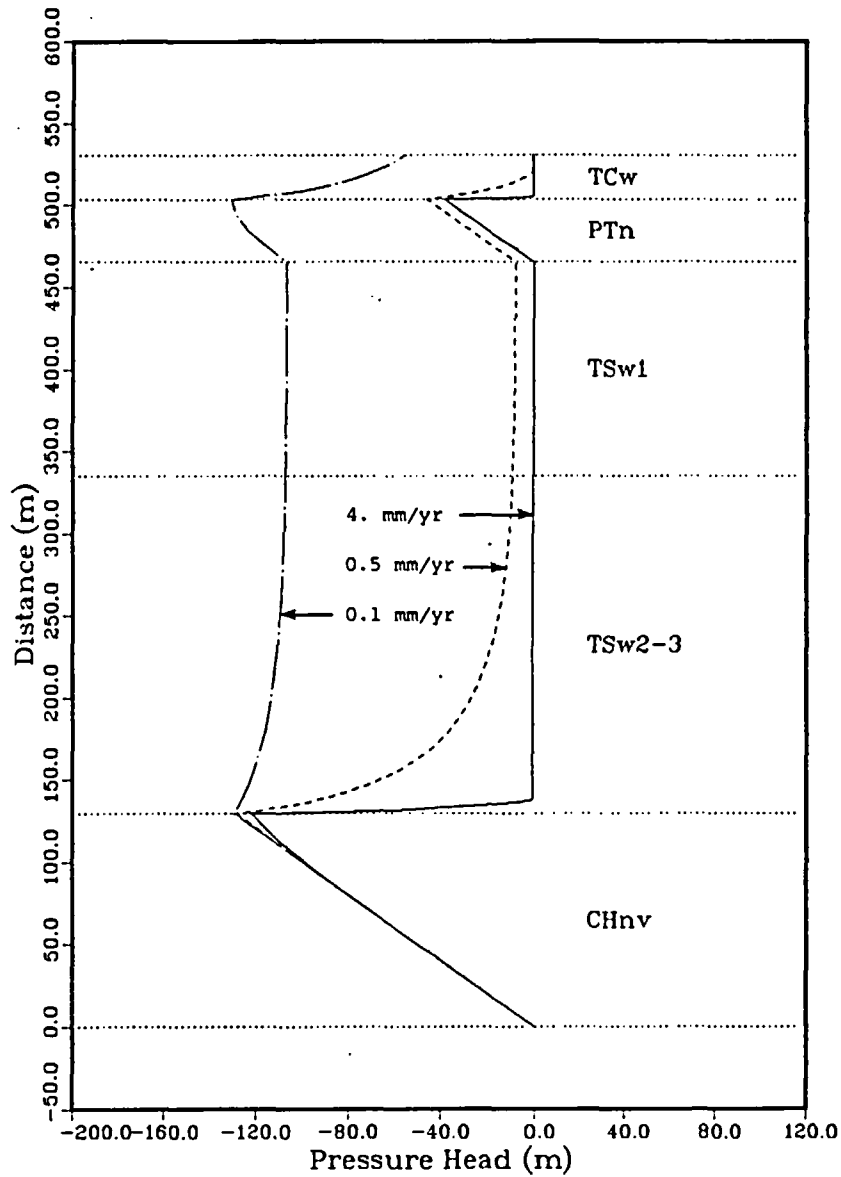


Figure 8. Pressure head versus distance above the water table for vitric unit CHn cases

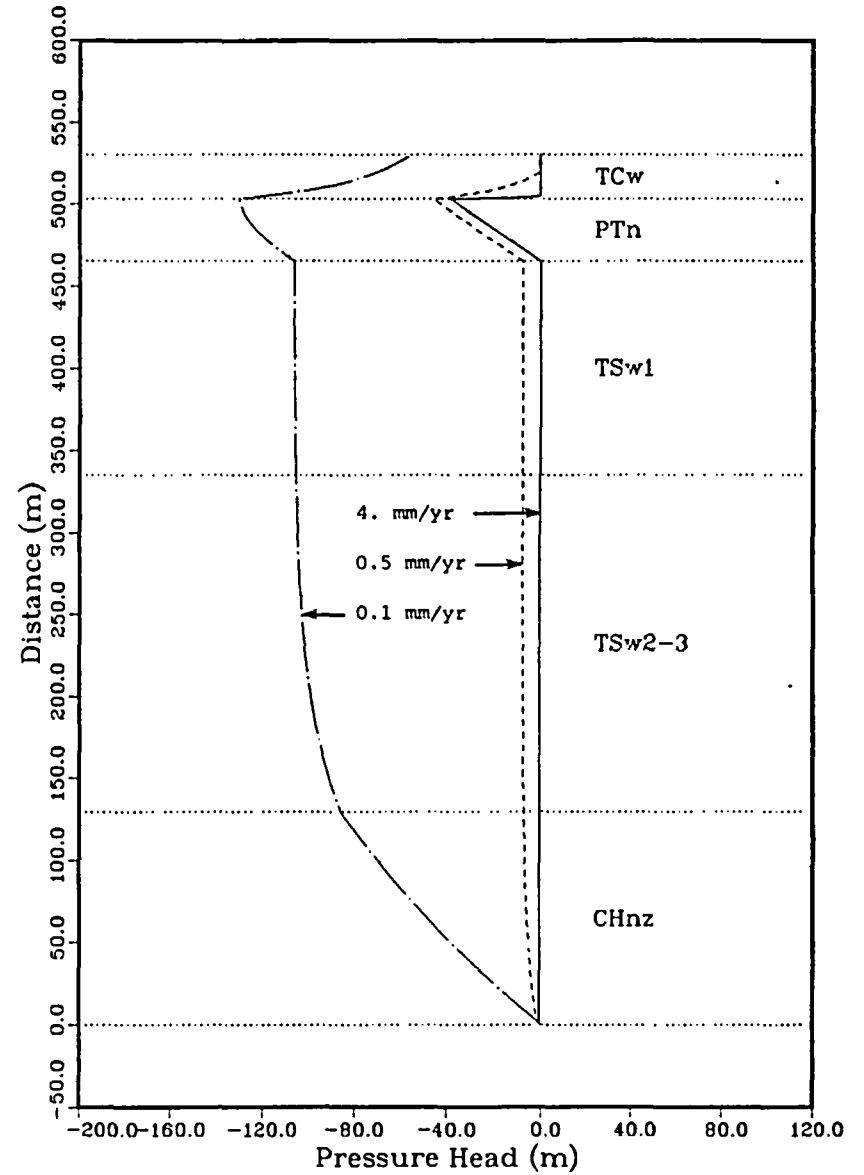


Figure 9. Pressure head versus distance above the water table for zeolitized unit CHn cases

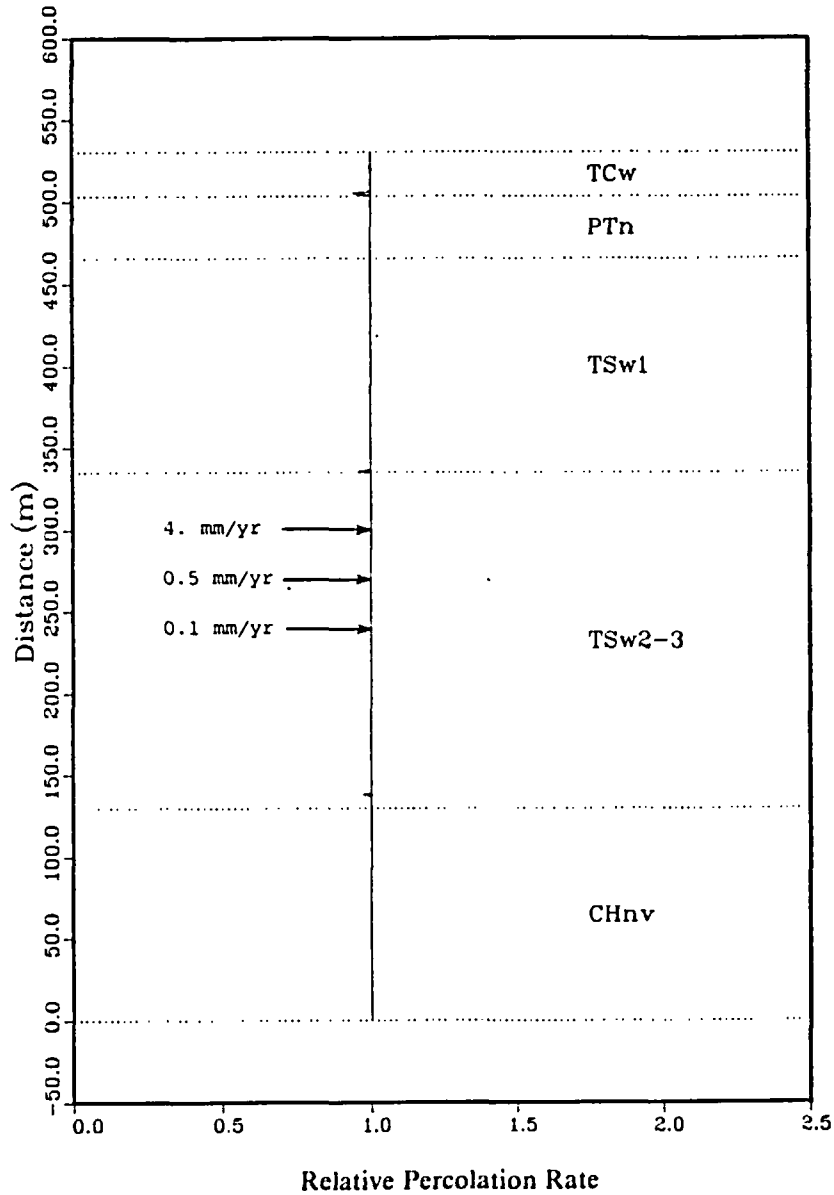


Figure 10. Relative percolation rate versus distance above the water table for vitric unit CHn cases; results are shown for three different percolation rates

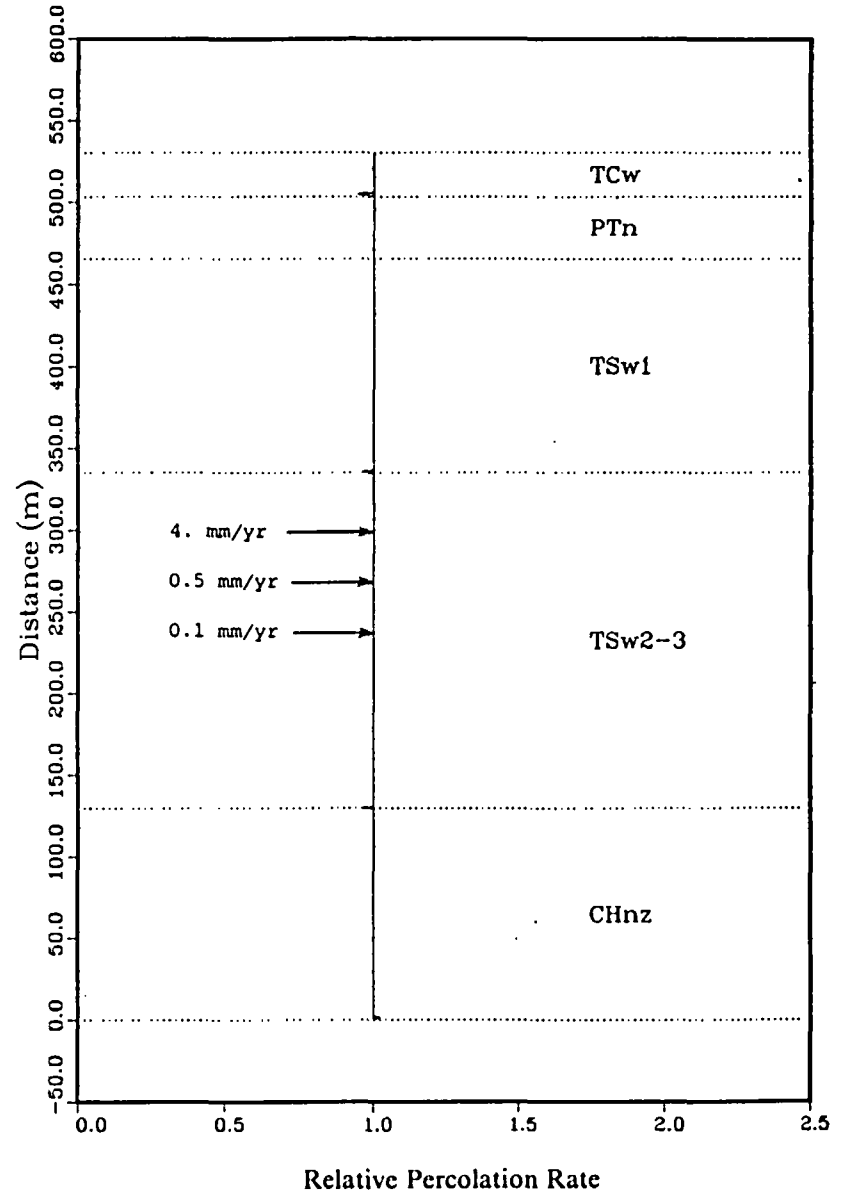


Figure 11. Relative percolation rate versus distance above the water table for zeolitized unit CHn cases; results are shown for three different percolation rates

pressure head in that unit is near zero; this indicates the matrix is saturated and the fractures are carrying significant amounts of water. If the saturated matrix conductivity is large compared to the percolation rate (e.g., the case where an imposed percolation rate of 4.0 mm/yr passes through vitric unit CHn, which has a saturated matrix conductivity of 8,400 mm/yr), then the pressure head drops off rapidly in an approximately linear fashion moving from a value of zero at the water table toward its lower limit, which is the pressure head where the conductivity equals the percolation rate. Finally, if the percolation rate is intermediate between the saturated conductivities of two adjacent units, then there will be a rapid and sometimes nearly discontinuous change in pressure head near the interface of the units. An example of this can be seen at the interface between unit CHnv (saturated matrix conductivity of 8,400 mm/yr) and unit TSw2-3 (saturated matrix conductivity of 0.6 mm/yr) for the case where the percolation rate is 4.0 mm/yr. As the percolation rate is reduced, this discontinuity may nearly disappear. Note the change in the shape of the curve at the interface of unit CHnv and unit TSw2-3 as the percolation rate is reduced to 0.1 mm/yr, which is less than the matrix conductivity of both units. Note also that the pressure head is zero at the bottom of the mesh, which is the location of the water table.

The saturated matrix conductivity of unit CHnz (0.6 mm/yr) is approximately the same as the percolation rates used in these calculations, while the saturated conductivity of unit CHnv is always much greater than the percolation rate. Therefore, for the same percolation rate, unit CHnz is more saturated (Figure 9) than CHnv (Figure 8) in order to carry the flux, and its pressure head is much closer to zero. At a percolation rate of 4.0 mm/yr, the pressure head in unit CHnz is nearly zero, indicating that both the matrix and fractures are carrying water.

Regions where the slope of the pressure head changes rapidly correspond to the regions where the calculated percolation rate does not match that imposed at the upper boundary. The place where problems occur most frequently is at the boundary between units that have very different saturated conductivities. The pressure-head profile at this location may change rapidly. An example of a rapid change in pressure-head profile

can be seen (Figure 8) at the interface of unit TCw and unit PTn, with a percolation rate of 4.0 mm/yr. Figures 10 and 11 show that the calculated percolation rate is in error close to this interface.

In a few cases, the influence of one unit extends into another unit (e.g., Figure 8 above the contact between unit CHnv and unit TSw2-3 with a percolation rate of 4.0 mm/yr). Thus, there may be a region of quickly changing slope in the pressure-head profile within a unit where the calculated percolation rate is in error (e.g., in Figure 8 this occurs above the interface of unit CHnv and TSw2-3).

The calculated percolation rate may therefore, be in error both at the boundary between units and within a unit in the region where the pressure head becomes asymptotic to the constant value seen in the remainder of the unit. In most cases, the error occurs over a very small range and is less than 5% of the percolation rate. The magnitude of the error and the vertical distance over which it occurs can be reduced and, in fact, eliminated by making the calculational mesh very fine at the places where large changes exist in the slope of the pressure-head curve.

Matrix Saturation

The calculated pressure-head profile was used to calculate matrix-saturation profiles (Figures 12 and 13). The matrix-saturation profile can be nearly discontinuous because of the rapid changes in pressure head necessary to keep the percolation rate constant through the units and because of unit-to-unit differences in the saturation curves. For a particular percolation rate, units CHnv and CHnz have much different saturations because of the difference in their saturated conductivities.

Water Velocity

Figure 14 shows the velocity of water movement in the matrix for the cases where unit CHn is vitric. Figure 12 shows, that for most cases, the matrix saturation of the units does not change much (e.g., 20% for

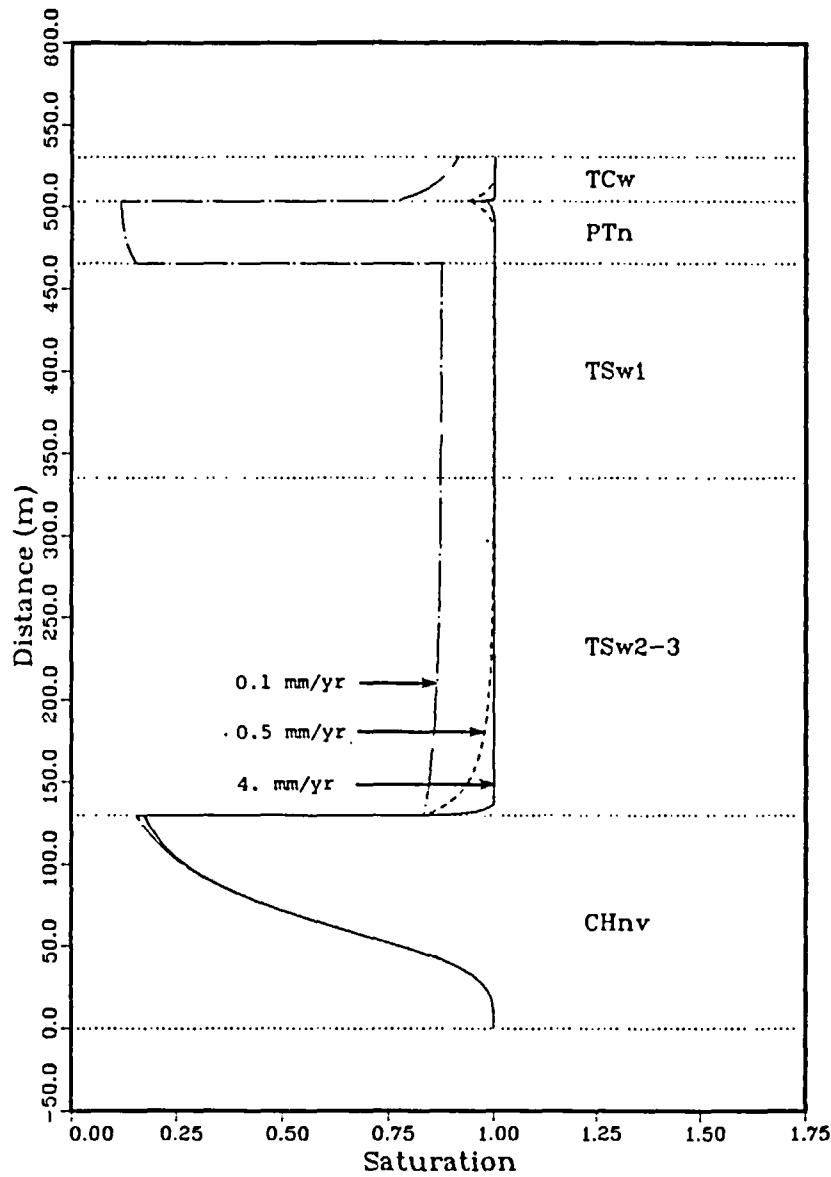


Figure 12. Matrix saturation versus distance above the water table for vitric unit CHn cases

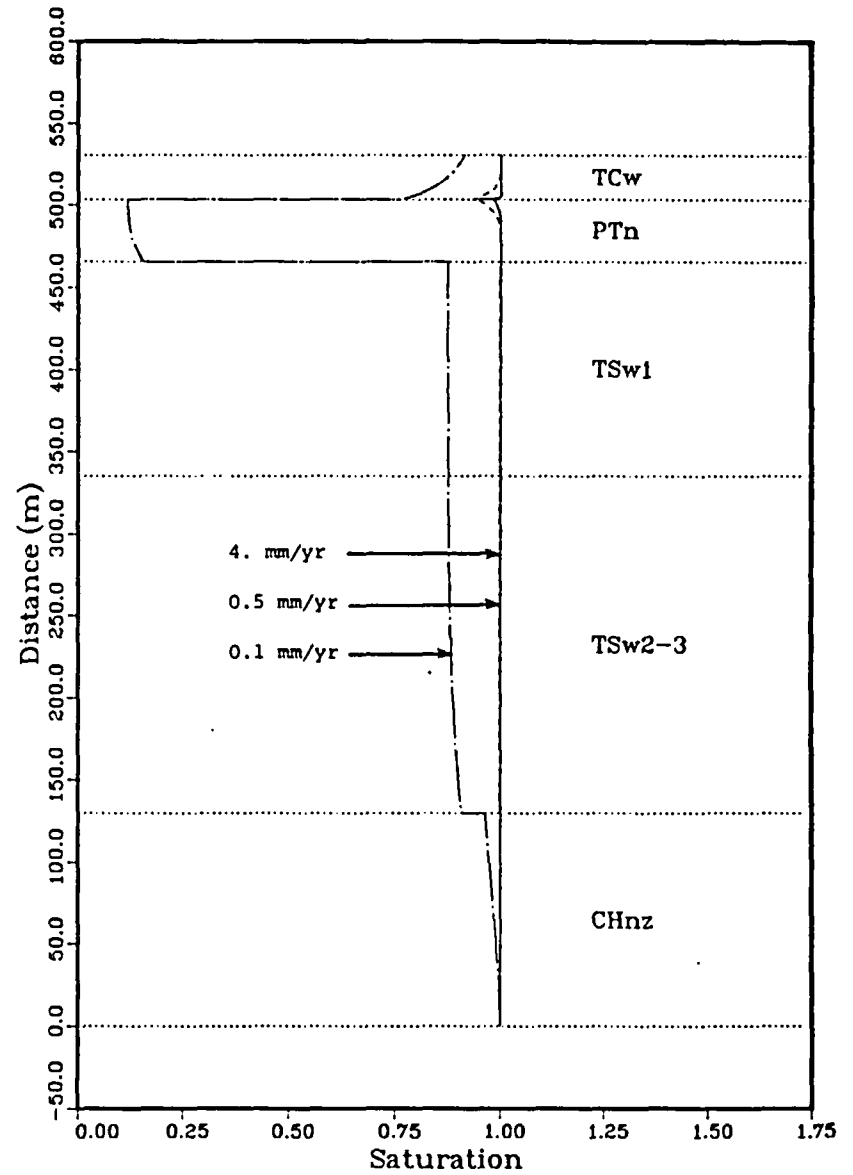


Figure 13. Matrix saturation versus distance above the water table for zeolitized unit CHn cases

unit TSw1) as the percolation rate is varied. Thus, Figure 14 shows, in general, that the matrix water velocity varies roughly linearly with the percolation rate until the matrix is nearly saturated (e.g., unit TSw1 for percolation rates of 0.1 and 0.5 mm/yr); then the velocity is nearly constant (e.g., unit TSw1 for percolation rates of 0.5 and 4.0 mm/yr) because the percolation rate in the matrix is nearly constant. The only unit that does not follow this general rule is PTn. At a percolation rate of 0.1 mm/yr, unit PTn's saturation is very low, resulting in a matrix water velocity which is large compared to that seen in the other units. At a percolation rate of 0.5 mm/yr, PTn is nearly saturated because of the influence of nearby units. Thus, the matrix water velocity has decreased relative to that at 0.1 mm/yr even though the percolation rate has increased. Finally, at a percolation rate of 4.0 mm/yr, the matrix water velocity has increased compared to that at a percolation rate of 0.5 mm/yr because the percolation rate has increased while the matrix saturation remained constant.

As previously discussed, the conductivity of the vitric unit CHn material is very large compared to both unit CHnz and the imposed percolation rates. Thus, for the same percolation rate, CHnv is much less saturated than CHnz. The matrix water velocity is an inverse function of the matrix saturation (Eq. 8). Thus, for the same percolation rate, the water velocity in CHnv is greater than that in CHnz (Figure 15).

Figures 16 and 17 show the velocity of water movement in the fractures for the CHnv and CHnz cases, respectively. In all cases, there is some water movement in the fractures near the water table (bottom of unit CHn) because the nearby water table keeps the pressure head near zero no matter what the percolation rate. At a percolation rate of 0.1 mm/yr there is no water movement in the fractures anywhere in the column except very near the water table. At a percolation rate of 0.5 mm/yr there is also water movement in the fractures in unit TCw, which has a saturated matrix conductivity of 0.3 mm/yr. The amount of water moving in the fractures drops to zero at the bottom of unit TCw because of the influence of unit PTn, which has a very high matrix conductivity and, to a certain extent, drains unit TCw. At a percolation rate of 4.0 mm/yr, all of the units with saturated matrix conductivities less than 4.0 mm/yr

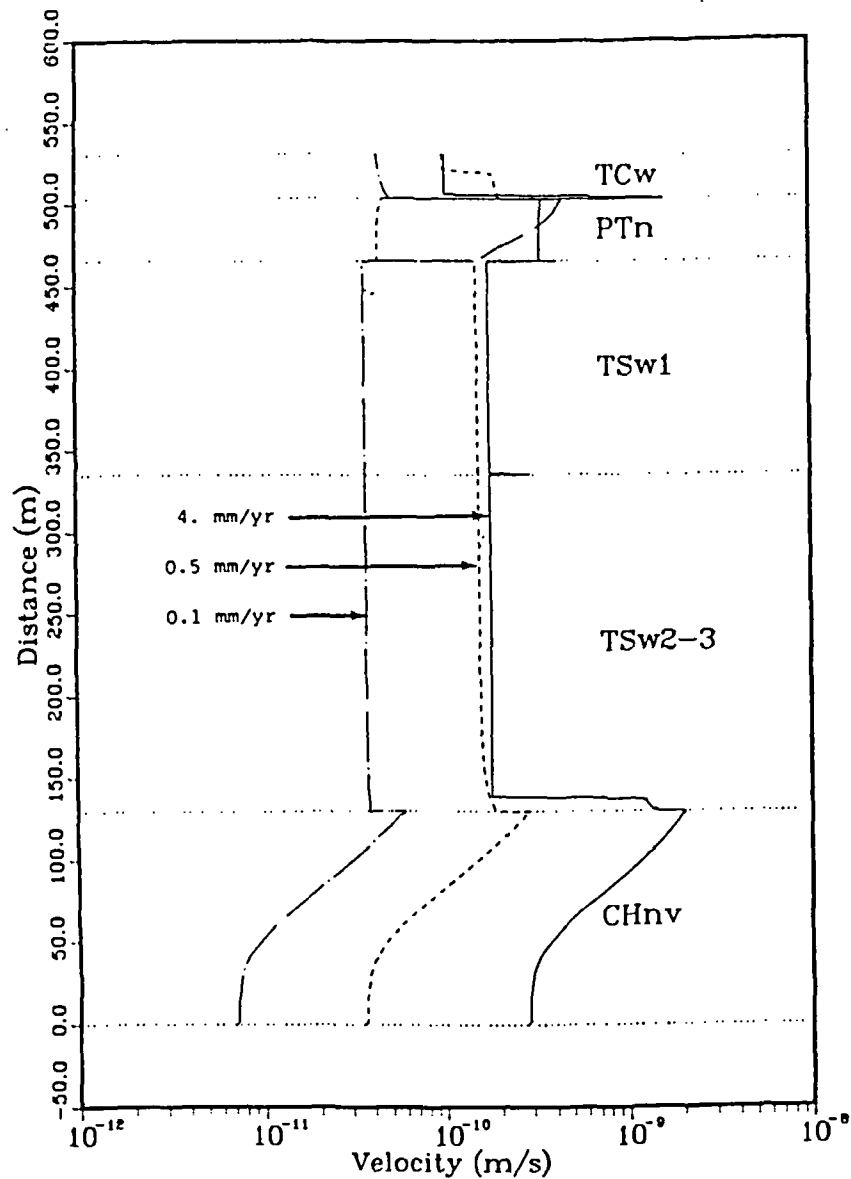


Figure 14. Water velocity in the matrix versus distance above the water table for vitric unit CHn cases

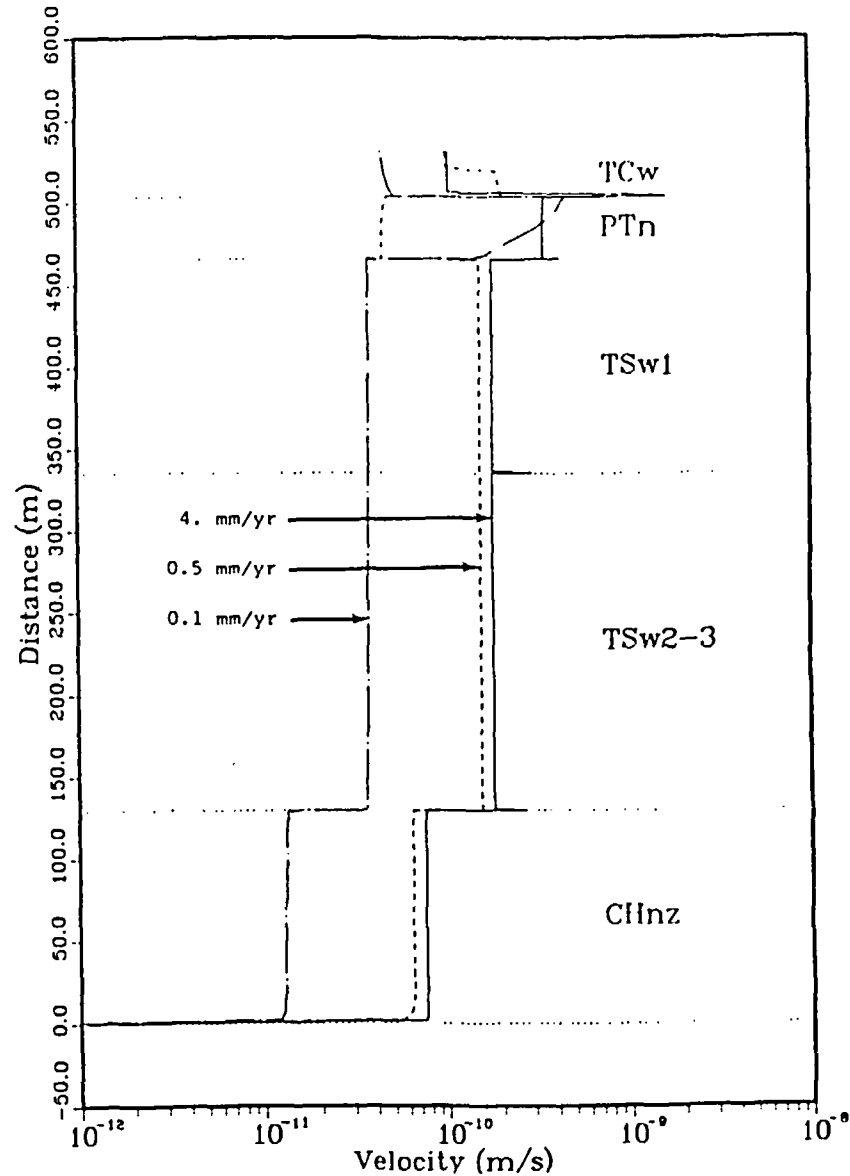


Figure 15. Water velocity in the matrix versus distance above the water table for zeolitized unit CHn cases

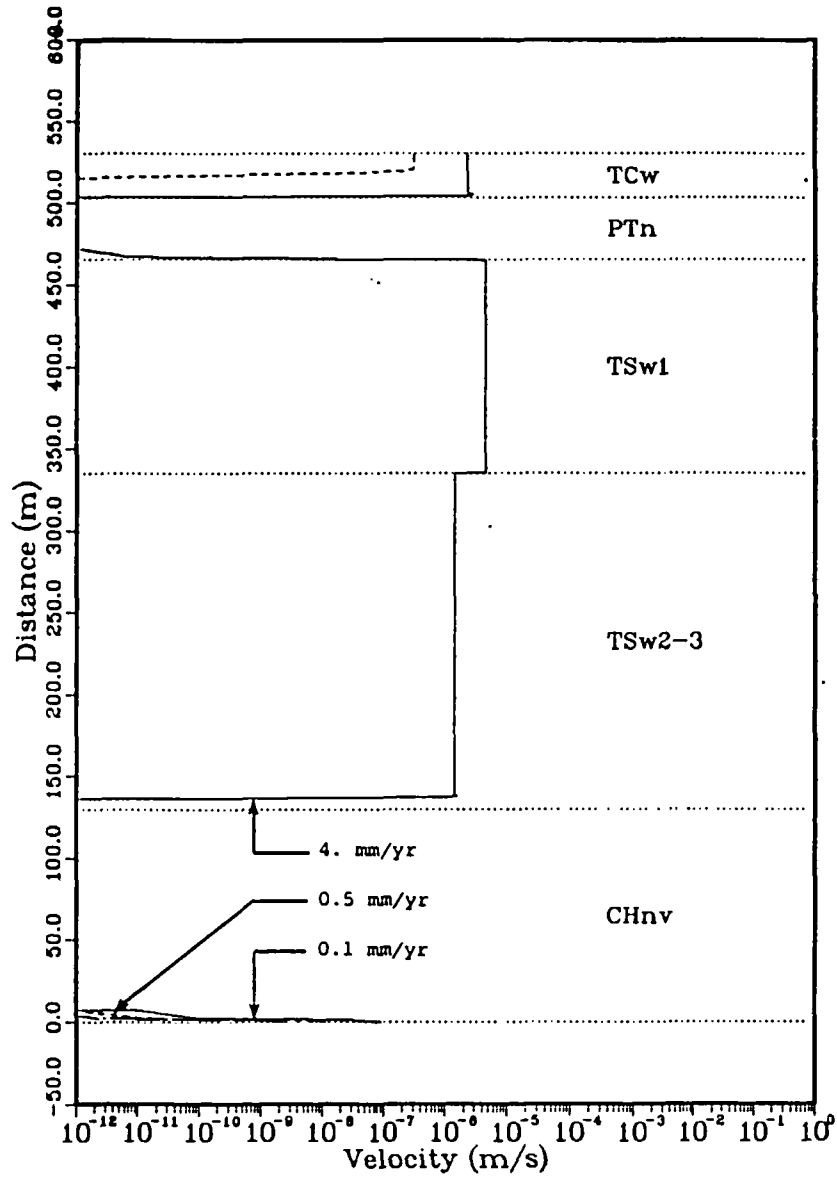


Figure 16. Water velocity in the fractures versus distance above the water table for vitric unit CHn cases

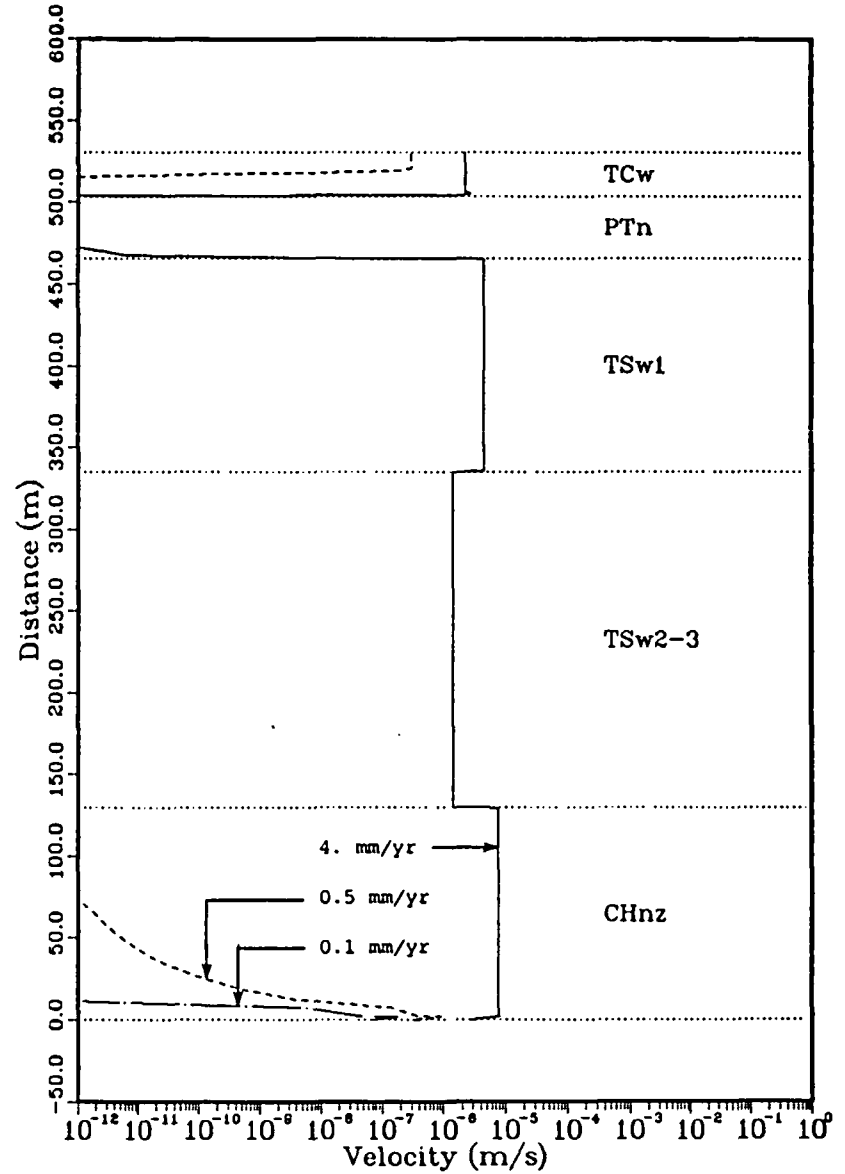


Figure 17. Water velocity in the fractures versus distance above the water table for zeolitized unit CHn cases

have water movement in fractures. Note that the velocities of the water moving in the fractures are much higher than those of water moving in the matrix, with the ratio being approximately equal to the reciprocal of the fracture porosity (of the order of 10^5).

A percolation rate of 4.0 mm/yr is greater than the saturated conductivity of CHnz but not that of CHnv. Thus, the major difference between the figures for units CHnz and CHnv is the fact that water movement occurs in the fractures in CHnz at a percolation rate of 4.0 mm/yr (Figure 17) while there is no water movement in the fractures of CHnv at this percolation rate (Figure 16).

Water Travel Time Across the Units at Yucca Mountain

Figures 18 through 23 show water travel times across each of the units in the column for all six of the cases investigated. These figures also show the travel time across the lower half of the prospective repository unit (TSw2-3) so that the travel time from the repository to the water table can be calculated.

In Figures 18 (vitric unit CHn) and 19 (zeolitized unit CHn), the percolation rate is 0.1 mm/yr, and the water flow is confined entirely to the matrix in all but one unit; thus, the minimum travel times across each of the units are very long. As previously discussed, there is water movement in the fractures near the water table no matter what the percolation rate. Figure 18 shows that it takes 11.2 yr for water in the fractures to cross 0.5% of unit CHnv. The water movement in the fractures near the water table causes the minimum travel time across unit CHn to be less than the matrix water travel time (329,000 and 332,000 yr, respectively). The major difference between Figures 18 and 19 is the travel time across unit CHn. This difference is, of course, due to the difference in water velocities in units CHnv and CHnz. The difference in velocities ultimately results from the difference in saturated matrix conductivities of units CHnv and CHnz; the discussion of Figures 14 and 15 is relevant here.

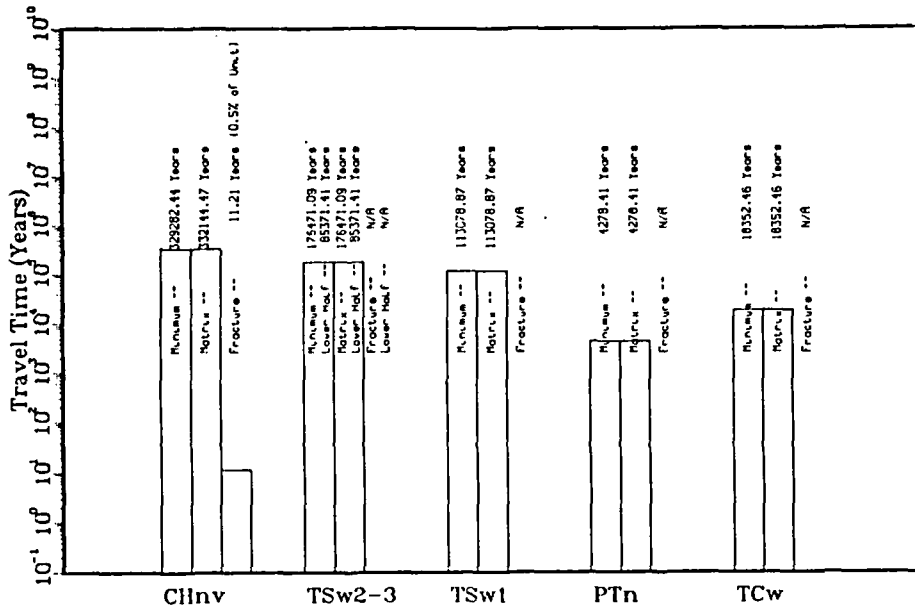


Figure 18. Water travel time across the units at Yucca Mountain for a vitric unit CHn and a percolation rate of 0.1 mm/yr

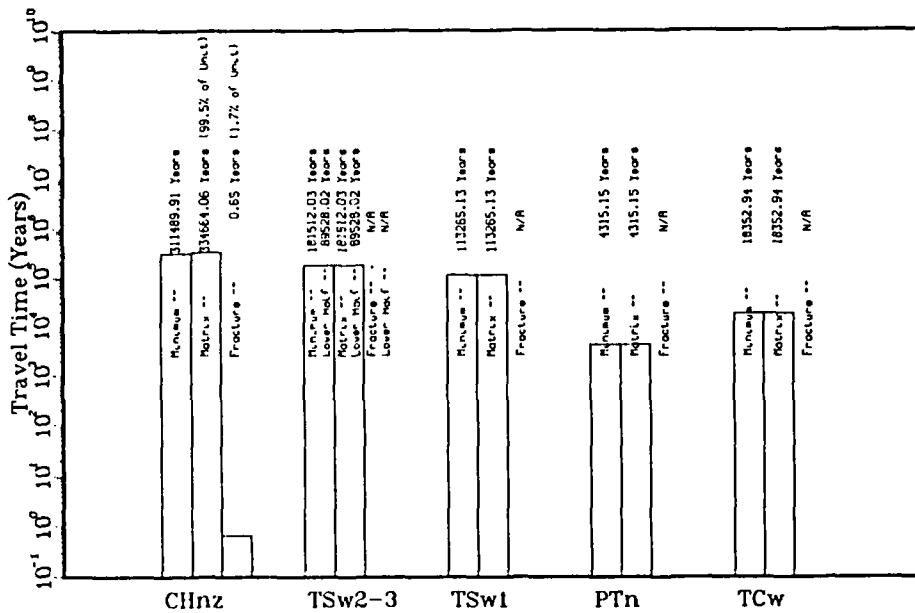


Figure 19. Water travel time across the units at Yucca Mountain for a zeolitized unit CHn and a percolation rate of 0.1 mm/yr

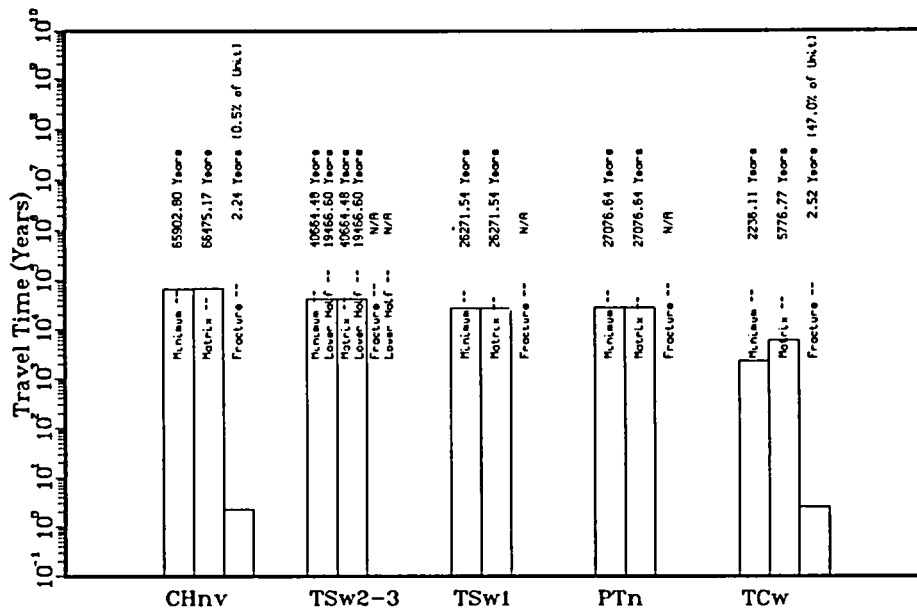


Figure 20. Water travel time across the units at Yucca Mountain for a vitric unit CHn and a percolation rate of 0.5 mm/yr

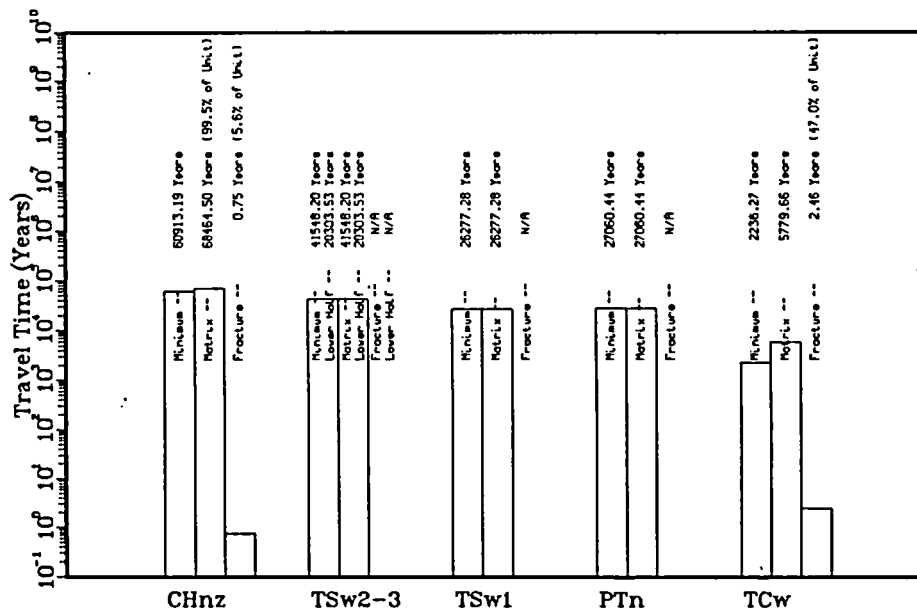


Figure 21. Water travel time across the units at Yucca Mountain for a zeolitized unit CHn and a percolation rate of 0.5 mm/yr

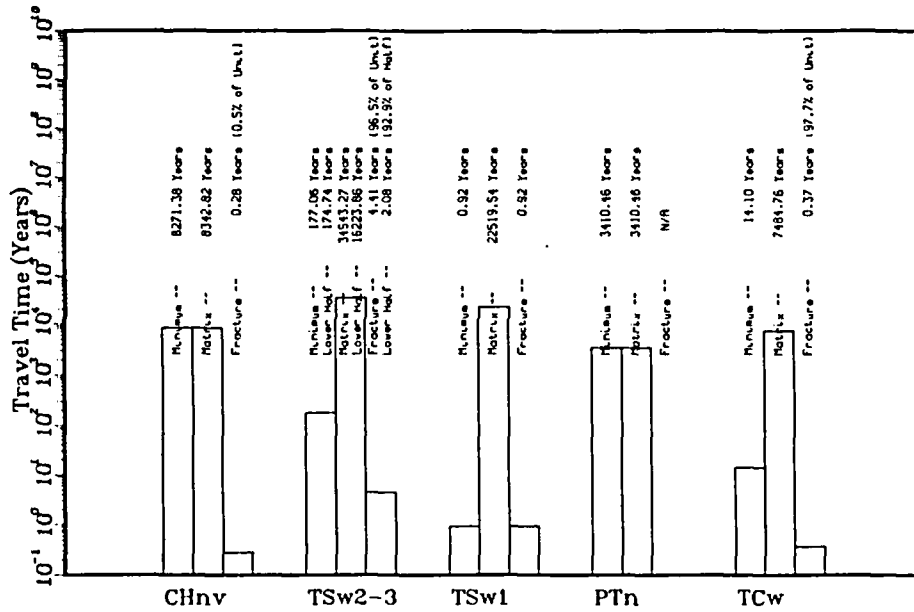


Figure 22. Water travel time across the units at Yucca Mountain for a vitric unit CHn and a percolation rate of 4.0 mm/yr

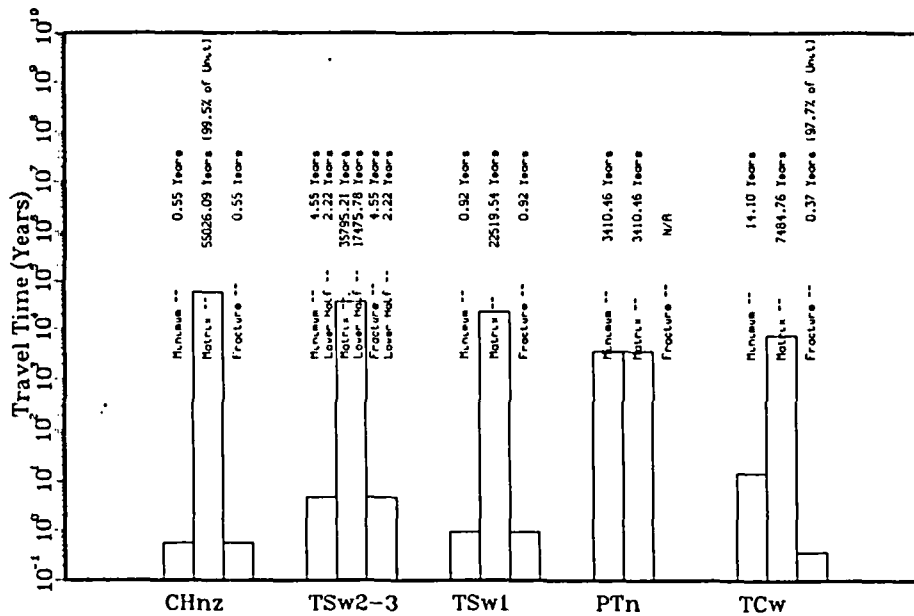


Figure 23. Water travel time across the units at Yucca Mountain for a zeolitized unit CHn and a percolation rate of 4.0 mm/yr

Figures 20 (CHnv) and 21 (CHnz) show the water travel times for a constant percolation rate of 0.5 mm/yr. The travel times across the units are approximately one-fifth that of the case where the percolation rate was 0.1 mm/yr. There are two exceptions to this observation. Unit TCw has substantial fracture flow at this percolation rate, and this affects the minimum water travel time across TCw. The second exception is unit PTn, which has a large change in matrix saturation that affects the velocity of water movement in the matrix. Therefore, the travel time across PTn increases as the percolation rate is increased to 0.5 mm/yr. The major difference between Figures 20 and 21 is the travel time across unit CHn, a matter that has been discussed previously. Because a percolation rate of 0.5 mm/yr is near the saturated conductivity of CHnz (0.6 mm/yr) the percentage of CHnz that has water movement in the fractures is somewhat larger than for the previous case where the percolation rate was 0.1 mm/yr.

At a percolation rate of 4.0 mm/yr (Figures 22 and 23), the water movement in fractures is substantial in units with relatively low matrix conductivities (TCw, TSw1, TSw2-3 and unit CHnz). The movement of water in fractures causes the minimum water travel time across each of these units to decrease dramatically compared to the two lower percolation rate cases. In most cases, the reduction is of the same order of magnitude as the fracture porosity. For example, with a percolation rate of 0.5 mm/yr the minimum water travel time across unit TSw1 is 26,000 yr; with a percolation rate of 4.0 mm/yr, the minimum water travel time is 1 yr. The ratio of the two travel times is approximately 10^{-5} , which is nearly the same as the fracture porosity. Units CHnv and CHnz have much different travel times because of their differences in saturated matrix conductivity.

The minimum water travel time from the prospective repository location (middle of unit TSw2-3) to the water table was calculated for each of the cases from the results shown in Figures 18 through 23; the results are listed in Table 3. They indicate that the percolation rate has a profound effect on this travel time primarily because of the initiation of water movement in fractures. For example, for the cases where unit CHn is zeolitized, water movement in fractures occurs in both unit TSw2-3 and unit CHn at a percolation rate of 4.0 mm/yr; the water

Table 3 Water travel time from the prospective repository location to the water table

<u>PERCOLATION RATE</u>	<u>TRAVEL TIME VITRIC UNIT CHn</u>	<u>TRAVEL TIME ZEOLITIZED UNIT CHn</u>
0.1 mm/yr	410,000 yr	400,000 yr
0.5 mm/yr	85,000 yr	81,000 yr
4.0 mm/yr	8,400 yr	3 yr

travel time from the repository to the water table drops by a factor of about 30,000 from the case where the percolation rate is 0.5 mm/yr and no water movement in the fractures occurs. In all but one of the cases studied, the water travel time from the repository to the water table is greater than 1,000 yr. In the case where the travel time is the shortest, two variables are set to extreme values; 1) the flux is at a very high value of 4.0 mm/yr and 2) the CHn unit is entirely zeolitized (in most of Yucca Mountain there is a vitric layer also). Current regulations require a minimum water travel time from the repository to the accessible environment of 1,000 yr. The boundary of the accessible environment has not been defined; it likely will not be the water table but instead the boundary will be downstream of the point of entry into the water table.

SUMMARY

The U.S. DOE is investigating the unsaturated zone at Yucca Mountain as a possible host for a radioactive-waste repository. The hydrologic units at Yucca Mountain can be grouped into three different types of rock. Two of these have relatively low matrix conductivities, and the third type has matrix conductivities that are very large in comparison to estimates of the percolation rate. The effects of percolation rate and the composition of hydrologic unit CHn on water movement in Yucca

Mountain have been estimated. The water travel time was shown to be sensitive to the percolation rate, with the greatest sensitivity shown to occur at the percolation rate where water movement in the fractures is initiated.

REFERENCES

- DOE. 1984. "Draft Environmental Assessment - Yucca Mountain Site, Nevada Research and Development Area, Nevada," U.S. Department of Energy, Washington, D.C.
- Dudley, A. L., R. R. Peters, M. S. Tierney, E. A. Klavetter, J. H. Gauthier, and M. Wilson. In preparation. "Total Systems Performance Assessment Code (TOSPAC) Volume 1: Physical and Mathematical Bases," SAND85-0002, Sandia National Laboratories, Albuquerque, NM.
- Freeze, R. A., and J. A. Cherry. 1979. "GROUNDWATER," Prentice-Hall, Inc., Englewood Cliffs, NJ.
- Klavetter, E. A., and R. R. Peters. 1985a. "Fluid Flow in Fractured Rock Masses," DOE/NRC Symposium on Groundwater Flow and Transport Modeling, May 20-21, Albuquerque, NM.
- Klavetter, E. A., and R. R. Peters. 1985b. "Estimation of Hydrologic Properties for an Unsaturated, Fractured Rock Mass," SAND84-2642, Sandia National Laboratories, Albuquerque, NM.
- Klavetter, E. A., R. R. Peters, and B. M. Schwartz. 1985. "Experimental Plan for Investigating Water Movement Through Fractures," SAND84-0468, Sandia National Laboratories, Albuquerque, NM.
- Martinez, M. J. In preparation. "Capillary Driven Flow in a Fracture Located in a Porous Media," SAND84-1697, Sandia National Laboratories, Albuquerque, NM.
- McTigue, D. F., R. K. Wilson, and J. W. Nunziato. 1984. "An Effective Stress Principle for Partially Saturated Media," SAND82-1977, Sandia National Laboratories, Albuquerque, NM.
- Mercer, J. 1983. "Role of the Unsaturated Zone in Radioactive and Hazardous Waste Disposal," Ann Arbor Science, Ann Arbor, MI.
- Montazer, P., and W. E. Wilson. 1984. "Conceptual Hydrologic Model of Flow in the Unsaturated Zone, Yucca Mountain, Nevada," Water-Resources Investigations Report 84-4345, U.S. Geological Survey, Denver, CO.
- Mualem, Y. 1976. "A New Model for Predicting the Hydraulic Conductivity of Unsaturated Porous Materials," Water Resources Research 12(3), pp. 513-522.
- Nimick, F. B., S. J. Bauer, and J. R. Tillerson. 1984. "Recommended Matrix and Rock-Matrix Bulk, Mechanical and Thermal Properties for Thermomechanical Stratigraphy of Yucca Mountain," Keystone Doc. 6310-85-1, Sandia National Laboratories, Albuquerque, NM.
- Ortiz, T. S., R. L. Williams, F. B. Nimick, B. C. Whittet, and D. L. South. 1985. "A Three-Dimensional Model of the Thermal-Mechanical Units at Yucca Mountain, Southern Nevada," SAND84-1076, Sandia National Laboratories, Albuquerque, NM.

- Peters, R. R., E. A. Klavetter, I. J. Hall, S. C. Blair, P. R. Heller, and G. W. Gee. 1984. "Fracture and Matrix Hydrologic Characteristics of Tuffaceous Materials from Yucca Mountain, Nye County, Nevada," SAND84-1471, Sandia National Laboratories, Albuquerque, NM.
- Reeves, M., and J. O. Duguid. 1975. "Water Movement Through Saturated-Unsaturated Porous Media: A Finite-Element Galerkin Model," ORNL-4927, Oak Ridge National Laboratory, Oak Ridge, TN.
- Reisenauer, A. E., K. T. Key, T. N. Narasimhan, and R. W. Nelson. 1982. "TRUST: A Computer Program for Variably Saturated Flow in Multidimensional, Deformable Media," NUREG/CR-2360, U.S. Nuclear Regulatory Commission, Washington, D.C.
- Richards, L. A. 1931. "Capillary Conduction of Liquids Through Porous Mediums [sic], Physics, Vol. 1, pp. 318-333.
- Roseboom, E. H., Jr. 1983. "Disposal of High-Level Nuclear Waste Above the Water Table in Arid Regions," U.S. Geological Survey Circular 903, Alexandria, VA.
- Ross, B. 1984. "A Conceptual Model of Deep Unsaturated Zones with Negligible Recharge," Water Resources Research, Vol. 20, No. 11, pp. 1627-1629.
- Rush, F. E. 1970. "Regional Ground-Water Systems in the Nevada Test Site Area, Nye, Lincoln, and Clark Counties, Nevada," Department of Conservation and Natural Resources, Water Resources--Reconnaissance Series Report 54, State of Nevada, Carson City.
- Scott, R. B., R. W. Spengler, A. R. Lappin, and M. P. Chornack. 1983. "Geologic Character of Tuffs in the Unsaturated Zone at Yucca Mountain, Southern Nevada," in "Role of the Unsaturated Zone in Radioactive and Hazardous Waste Disposal," edited by J. Mercer, Ann Arbor Science, Ann Arbor, MI.
- Sinnock, S., Y. T. Lin, and J. P. Brannen. 1984. "Preliminary Bounds on the Expected Postclosure Performance of the Yucca Mountain Repository Site, Southern Nevada," SAND84-1492, Sandia National Laboratories, Albuquerque, NM.
- Travis, B. J., S. W. Hodson, H. E. Nuttal, T. L. Cook, and R. S. Rundberg. 1984. "Preliminary Estimates of Water Flow and Radionuclide Transport in Yucca Mountain," Mat. Res. Soc. Symp. Proc., Vol. 26, pp. 1039-1047.
- van Genuchten, R. 1978. "Calculating the Unsaturated Hydraulic Conductivity with a New Closed Form Analytical Model," Water Resources Bulletin, Princeton University Press, Princeton University, Princeton, NJ.

Wang, J. S. Y., and T. N. Narasimhan. 1985. "Hydrologic Mechanisms Governing Fluid Flow in Partially Saturated, Fractured, Porous Tuff at Yucca Mountain," SAND84-7202, Sandia National Laboratories, Albuquerque, NM.

Winograd, I. J. 1981. "Radioactive Waste Disposal in Thick Unsaturated Zones," Science, Vol. 212, pp. 1457-1464.

DISTRIBUTION LIST

B. C. Rusche (RW-1)
Director
Office of Civilian Radioactive
Waste Management
U.S. Department of Energy
Forrestal Building
Washington, DC 20585

Ralph Stein (RW-23)
Office of Geologic Repositories
U.S. Department of Energy
Forrestal Building
Washington, DC 20585

J. J. Fiore, (RW-22)
Program Management Division
Office of Geologic Repositories
U.S. Department of Energy
Forrestal Building
Washington, DC 20585

M. W. Frei (RW-23)
Engineering & Licensing Division
Office of Geologic Repositories
U.S. Department of Energy
Forrestal Building
Washington, DC 20585

E. S. Burton (RW-25)
Siting Division
Office of Geologic Repositories
U.S. Department of Energy
Forrestal Building
Washington, D.C. 20585

C. R. Cooley (RW-24)
Geosciences & Technology Division
Office of Geologic Repositories
U.S. Department of Energy
Forrestal Building
Washington, DC 20585

V. J. Cassella (RW-22)
Office of Geologic Repositories
U.S. Department of Energy
Forrestal Building
Washington, DC 20585

T. P. Longo (RW-25)
Program Management Division
Office of Geologic Repositories
U.S. Department of Energy
Forrestal Building
Washington, DC 20585

Cy Klingsberg (RW-24)
Geosciences and Technology Division
Office of Geologic Repositories
U. S. Department of Energy
Forrestal Building
Washington, DC 20585

B. G. Gale (RW-25)
Siting Division
Office of Geologic Repositories
U.S. Department of Energy
Forrestal Building
Washington, D.C. 20585

R. J. Blaney (RW-22)
Program Management Division
Office of Geologic Repositories
U.S. Department of Energy
Forrestal Building
Washington, DC 20585

R. W. Gale (RW-40)
Office of Policy, Integration, and
Outreach
U.S. Department of Energy
Forrestal Building
Washington, D.C. 20585

J. E. Shaheen (RW-44)
Outreach Programs
Office of Policy, Integration and
Outreach
U.S. Department of Energy
Forrestal Building
Washington, DC 20585

J. O. Neff, Manager
Salt Repository Project Office
U.S. Department of Energy
505 King Avenue
Columbus, OH 43201

D. C. Newton (RW-23)
Engineering & Licensing Division
Office of Geologic Repositories
U.S. Department of Energy
Forrestal Building
Washington, DC 20585

S. A. Mann, Manager
Crystalline Rock Project Office
U.S. Department of Energy
9800 South Cass Avenue
Argonne, IL 60439

O. L. Olson, Manager
Basalt Waste Isolation Project Office
U.S. Department of Energy
Richland Operations Office
Post Office Box 550
Richland, WA 99352

K. Street, Jr.
Lawrence Livermore National
Laboratory
Post Office Box 808
Mail Stop L-209
Livermore, CA 94550

D. L. Vieth, Director (4)
Waste Management Project Office
U.S. Department of Energy
Post Office Box 14100
Las Vegas, NV 89114

L. D. Ramspott (3)
Technical Project Officer for NNWSI
Lawrence Livermore National
Laboratory
P.O. Box 808
Mail Stop L-204
Livermore, CA 94550

D. F. Miller, Director
Office of Public Affairs
U.S. Department of Energy
Post Office Box 14100
Las Vegas, NV 89114

W. J. Purcell (RW-20)
Office of Geologic Repositories
U.S. Department of Energy
Forrestal Building
Washington, DC 20585

D. A. Nowack (12)
Office of Public Affairs
U.S. Department of Energy
Post Office Box 14100
Las Vegas, NV 89114

D. T. Oakley (4)
Technical Project Officer for NNWSI
Los Alamos National Laboratory
P.O. Box 1663
Mail Stop F-619
Los Alamos, NM 87545

B. W. Church, Director
Health Physics Division
U.S. Department of Energy
Post Office Box 14100
Las Vegas, NV 89114

W. W. Dudley, Jr. (3)
Technical Project Officer for NNWSI
U.S. Geological Survey
Post Office Box 25046
418 Federal Center
Denver, CO 80225

Chief, Repository Projects Branch
Division of Waste Management
U.S. Nuclear Regulatory Commission
Washington, D.C. 20555

NTS Section Leader
Repository Project Branch
Division of Waste Management
U.S. Nuclear Regulatory Commission
Washington, D.C. 20555

Document Control Center
Division of Waste Management
U.S. Nuclear Regulatory Commission
Washington, D.C. 20555

V. M. Glanzman
U.S. Geological Survey
Post Office Box 25046
913 Federal Center
Denver, CO 80225

P. T. Prestholt
NRC Site Representative
1050 East Flamingo Road
Suite 319
Las Vegas, NV 89109

J. S. Wright
Technical Project Officer for NNWSI
Westinghouse Electric Corporation
Waste Technology Services Division
Nevada Operations
Post Office Box 708
Mail Stop 703
Mercury, NV 89023

M. E. Spaeth
Technical Project Officer for NNWSI
Science Applications
International, Corporation
2769 South Highland Drive
Las Vegas, NV 89109

ONWI Library
Battelle Columbus Laboratory
Office of Nuclear Waste Isolation
505 King Avenue
Columbus, OH 43201

SAIC-T&MSS Library (2)
Science Applications
International, Corporation
2950 South Highland Drive
Las Vegas, NV 89109

W. M. Hewitt, Program Manager
Roy F. Weston, Inc.
2301 Research Blvd., 3rd Floor
Rockville, MD 20850

W. S. Twenhofel, Consultant
Science Applications
International, Corp.
820 Estes Street
Lakewood, CO 80215

H. D. Cunningham
General Manager
Reynolds Electrical &
Engineering Co., Inc.
Post Office Box 14400
Mail Stop 555
Las Vegas, NV 89114

A. E. Gurrola
General Manager
Energy Support Division
Holmes & Narver, Inc.
Post Office Box 14340
Las Vegas, NV 89114

T. Hay, Executive Assistant
Office of the Governor
State of Nevada
Capitol Complex
Carson City, NV 89710

J. A. Cross, Manager
Las Vegas Branch
Fenix & Scisson, Inc.
Post Office Box 15408
Las Vegas, NV 89114

R. R. Loux, Jr., Director (3)
Nuclear Waste Project Office
State of Nevada
Capitol Complex
Carson City, NV 89710

Neal Duncan (RW-44)
Office of Policy, Integration, and
Outreach
U.S. Department of Energy
Forrestal Building
Washington, DC 20585

C. H. Johnson, Technical
Program Manager
Nuclear Waste Project Office
State of Nevada
Capitol Complex
Carson City, NV 89710

John Fordham
Desert Research Institute
Water Resources Center
Post Office Box 60220
Reno, NV 89506

Department of Comprehensive
Planning
Clark County
225 Bridger Avenue, 7th Floor
Las Vegas, NV 89155

Lincoln County Commission
Lincoln County
Post Office Box 90
Pioche, NV 89043

Community Planning and
Development
City of North Las Vegas
Post Office Box 4086
North Las Vegas, NV 89030

City Manager
City of Henderson
Henderson, NV 89015

N. A. Norman
Project Manager
Bechtel National Inc.
P. O. Box 3965
San Francisco, CA 94119

Flo Butler
Los Alamos Technical Associates
1650 Trinity Drive
Los Alamos, New Mexico 87544

Timothy G. Barbour
Science Applications
International Corporation
1626 Cole Boulevard, Suite 270
Golden, CO 80401

Dr. Martin Mifflin
Desert Research Institute
Water Resources Center
Suite 1
2505 Chandler Avenue
Las Vegas, NV 89120

Planning Department
Nye County
Post Office Box 153
Tonopah, NV 89049

Economic Development
Department
City of Las Vegas
400 East Stewart Avenue
Las Vegas, NV 89101

Director of Community
Planning
City of Boulder City
Post Office Box 367
Boulder City, NV 89005

Commission of the
European Communities
200 Rue de la Loi
B-1049 Brussels
BELGIUM

Technical Information Center
Roy F. Weston, Inc.
2301 Research Boulevard,
Third Floor
Rockville, MD 20850

R. Harig
Parsons Brinkerhoff Quade &
Douglas, Inc.
1625 Van Ness Ave.
San Francisco, CA 94109-3678

Dr. Madan M. Singh, President
Engineers International, Inc.
98 East Naperville Road
Westmont, IL 60559-1595

E. P. Binnall
Field Systems Group Leader
Building 50B/4235
Lawrence Berkeley Laboratory
Berkeley, CA 94720

J. E. Gale
Groundwater Research Inst.
Dept. of Earth Sciences
U. of Waterloo
Waterloo, Ontario
Canada
N2L 3G1

D. Hodgkinson
Theoretical Physics Div.
AERE Harwell
Oxfordshire OX11 0RA
United Kingdom

R. B. Lyon
Acting Dir., Nuclear Fuel
Waste Management
Atomic Energy of Canada, Ltd.
Pinawa, Manitoba ROE 1LO
Canada

P. Raimbault
CEA/PSH
SAED/SASICC-DAS
CEN FAR BP.6
92260 Fonteney aux Roses
France

R. Codell
U.S. NRC
Washington, D.C. 20555

G. Dagen
Dept. of Mech. and Env.
Engineering
U. of California
Santa Barbara, CA 93106

F. H. Dove
Pacific Northwest Laboratory
P. O. Box 999
Richland, WA 99352

Roger Hart
Itasca Consulting Group, Inc.
P.O. Box 14806
Minneapolis, Minnesota 55414

A. Herbert
AERE Harwell
Oxfordshire OX11 0RA
United Kingdom

A. Larsson
Swedish Nuclear Power Inspectorate
Box 27106
S-102 52 Stockholm, Sweden

I. Neretnieks
Dept. Chemical Engineering
Royal Institute of Technology
S-10044 Stockholm, Sweden

D. Alexander
RW24 OCRWM
7F088 Forrestal Building
Washington, D.C. 20585

C. Cole
Pacific Northwest Laboratory
P.O. Box 999
Richland, WA 99352

S. Davis
Dept. of Hydrology and Water Res.
U. of Arizona
Tucson, AZ 85719

K. Eggert
Lawrence Livermore Nat.
Laboratories
P. O. Box 808 L206
Livermore, CA 94550

D. Evans
Dept. of Hydrology and Water Res.
U. of Arizona
Tucson, AZ 85719

D.R.F. Harleman
Ford Professor of Engineering
Massachusetts Institute of
Technology
Cambridge, MA 02139

S. Key
Re/Spec Inc.
Box 1984
3515 Eubank NE
Albuquerque, NM 87191

P. Montazer
USGS-WRD, Mail Stop 416
Federal Center
Denver, CO 80225

S. Neuman
Dept. of Hydrology and Water Res.
U. of Arizona
Tucson, AZ 85719

W.W. Owens
6269 S. Knoxville
Tulsa, OK 74136

G. Pinder
Princeton University
Civil Engineering Dept.
Princeton, NJ

B. Ross
Disposal Safety Inc.
1211 Conn. Ave. NW
Suite 610
Washington, D.C. 20036

D. Stevens
Dept. of Soil Sciences
NM. Tech.
Socorro, NM 87801

D. T. Hoxie
U.S. Geological Survey
MS 416, Box 25046
Denver Federal Center
Denver, CO 80225

G. W. Gee
Pacific Northwest Laboratory
P.O. Box 999
Richland, WA 99352

P. Kelsall
IT Corporation
2340 S. Alamo
Albuquerque, NM 87106

J. A. Lieberman
OTHA, Inc.
P. O. Box 651
Glen Echo, MD 20812

T. N. Narasimhan
Lawrence Berkeley Laboratories
U. of California
Berkeley, CA 97420

T. J. Nicholson
Earth Sci. Branch
USNRC Mail Stop 1130-55
Washington, D.C. 20815

T. R. Pigford
Dept of Nuclear Engineering
U. of California
Berkeley, CA 94720

K. Pruess
Lawrence Berkeley Laboratories
Berkeley, CA 97420

R. Rulon
Lawrence Berkeley Laboratories
Berkeley, CA 97420

M. Teubner
Science Applications International
Corporation
Valley Bank Center
101 Convention Center Dr.
Suite 407
Las Vegas, NV 89109

B. J. Travis
Los Alamos Nat. Laboratory
P. O. Box 1663
Los Alamos, NM 87545

J. S. Y. Wang
Earth Science Division
Lawrence Berkeley Laboratories
Berkeley, CA 97420

D. T. Hoxie
U.S. Geological Survey
MS 416, Box 25046
Denver Federal Center
Denver, CO 80225

1511 N. E. Bixler
1511 R. R. Eaton
6300 R. W. Lynch
6310 T. O. Hunter
6310 CF 72-12144-1.6/NQ
6311 L. W. Scully
6311 C. Mora
6312 G. E. Barr
6312 F. W. Bingham
6312 A. L. Dudley
6312 J. H. Gauthier
6312 N. K. Hayden
6312 B. S. Langkopf
6312 R. R. Peters (20)
6312 R. W. Prindle
6312 M. S. Tierney
6312 M. Wilson
6312 J. G. Yeager
6313 T. E. Blejwas
6313 E. A. Klavetter (20)
6313 F. B. Nimick
6313 R. M. Zimmerman
6314 J. A. Fernandez
6314 J. R. Tillerson
6315 Y. T. Lin
6315 S. Sinnock
6331 A. R. Lappin
6332 WMT Library (20)
6430 N. R. Ortiz
6431 E. J. Bonano
6431 R. M. Cranwell
6431 R. Guzowski
7223 R. G. Easterling
7223 F. W. Spencer
7223 I. J. Hall
3141 S. A. Landenberger (5)
3151 W. L. Garner (3)
8024 P. W. Dean
3154-3 C. H. Dalin (28)
for DOE/OSTI

S. Tyler
DRI
2505 Chandler Ave., Suite 1
Las Vegas, NV 89120

W. E. Wilson
USGS-WRD, Mail Stop 416
Federal Center
Denver, CO 80225

G. S. Bodvarsson
Lawrence Berkeley Laboratory
Berkeley, CA 97420

